



Review

Recent Development and Future Prospective of Tiwari and Das Mathematical Model in Nanofluid Flow for Different Geometries: A Review

Mudasar Zafar ^{1,2,*}, Hamzah Sakidin ¹, Mikhail Sheremet ³, Iskandar B. Dzulkarnain ^{2,4}, Abida Hussain ¹, Roslinda Nazar ⁵, Javed Akbar Khan ⁶, Muhammad Irfan ⁷, Zafar Said ^{8,9,10}, Farkhanda Afzal ¹¹ and Abdullah Al-Yaari ¹

- Department of Fundamental and Applied Sciences, Universiti Teknologi PETRONAS, Bandar Seri Iskandar 32610, Perak, Malaysia
- Centre for Research in Enhanced Oil Recovery, Universiti Teknologi PETRONAS, Bandar Seri Iskandar 32610, Perak, Malaysia
- Laboratory on Convective Heat and Mass Transfer, Tomsk State University, 634050 Tomsk, Russia
- Department of Petroleum Engineering, Universiti Teknologi PETRONAS, Bandar Seri Iskandar 32610, Perak, Malaysia
- Department of Mathematical Sciences, Faculty of Science and Technology, Universiti Kebangsaan Malaysia, (UKM) Bangi 43600, Selangor, Malaysia
- Institute of Hydrocarbon Recovery, Universiti Teknologi PETRONAS, Bandar Seri Iskandar 32610, Perak, Malaysia
- ⁷ Electrical Engineering Department, College of Engineering, Najran University, Najran 61441, Saudi Arabia
- Sustainable and Renewable Energy Engineering College of Engineering, University of Sharjah, Sharjah 27272, United Arab Emirates
- ⁹ U.S.-Pakistan Centre for Advanced Studies in Energy (USPCAS-E), National University of Sciences and Technology (NUST), H-12, Islamabad 44000, Pakistan
- Department of Industrial and Mechanical Engineering, Lebanese American University (LAU), Byblos P.O. Box 13-5053, Lebanon
- Department of Humanities and Basic Sciences, MCS, National University of Sciences and Technology (NUST), Islamabad 44000, Pakistan
- * Correspondence: mudasar_20000296@utp.edu.my

Abstract: The rapid changes in nanotechnology over the last ten years have given scientists and engineers a lot of new things to study. The nanofluid constitutes one of the most significant advantages that has come out of all these improvements. Nanofluids, colloid suspensions of metallic and nonmetallic nanoparticles in common base fluids, are known for their astonishing ability to transfer heat. Previous research has focused on developing mathematical models and using varied geometries in nanofluids to boost heat transfer rates. However, an accurate mathematical model is another important factor that must be considered because it dramatically affects how heat flows. As a result, before using nanofluids for real-world heat transfer applications, a mathematical model should be used. This article provides a brief overview of the Tiwari and Das nanofluid models. Moreover, the effects of different geometries, nanoparticles, and their physical properties, such as viscosity, thermal conductivity, and heat capacity, as well as the role of cavities in entropy generation, are studied. The review also discusses the correlations used to predict nanofluids' thermophysical properties. The main goal of this review was to look at the different shapes used in convective heat transfer in more detail. It is observed that aluminium and copper nanoparticles provide better heat transfer rates in the cavity using the Tiwari and the Das nanofluid model. When compared to the base fluid, the Al₂O₃/water nanofluid's performance is improved by 6.09%. The inclination angle of the cavity as well as the periodic thermal boundary conditions can be used to effectively manage the parameters for heat and fluid flow inside the cavity.

Keywords: nanofluids; hybrid nanofluids; mathematical modeling geometries; convective heat transfer; entropy generation



Citation: Zafar, M.; Sakidin, H.; Sheremet, M.; Dzulkarnain, I.B.; Hussain, A.; Nazar, R.; Khan, J.A.; Irfan, M.; Said, Z.; Afzal, F.; et al. Recent Development and Future Prospective of Tiwari and Das Mathematical Model in Nanofluid Flow for Different Geometries: A Review. *Processes* 2023, 11, 834. https://doi.org/10.3390/pr11030834

Academic Editor: Gianpiero Colangelo

Received: 11 November 2022 Revised: 8 December 2022 Accepted: 27 December 2022 Published: 10 March 2023



Copyright: © 2023 by the authors. Licensee MDPI, Basel, Switzerland. This article is an open access article distributed under the terms and conditions of the Creative Commons Attribution (CC BY) license (https://creativecommons.org/licenses/by/4.0/).

Processes 2023, 11, 834 2 of 24

1. Introduction

Researchers have worked to comprehend the structure of nanofluids, evaluate their heat transfer ability, and analyze their heat transmission mechanisms. Nanofluids consist of a base fluid and a low volume percentage (between 1% and 10%) of solid particles with diameters typically less than 100 nm.

Oil, water, and ethylene glycol blends, which are commonly used as heat transfer fluids, are inefficient heat transfer fluids due to the thermal conductivity of the fluid, which in turn reduces the heat transfer coefficient between the fluid and the heat transfer surface.

Nanofluids possess unique thermal transport abilities and performance characteristics not found in conventional heat transfer fluids. Nanofluids have the potential to increase the heat transfer rates in solar collectors, nuclear reactors, and automobile radiators in comparison to standard solid–liquid suspensions, for these reasons [1,2]:

- The large surface area for heat transfer among the nanoparticles and the fluid implies a high effective thermal conductivity.
- The particles move in a dominating Brownian motion, resulting in a high dispersion stability.
- The pumping power is limited to obtain the same heat transfer intensification as pure liquid.
- The conventional slurries are less susceptible to particle blockage, making them appropriate for application in microsystems.
- The changes in particle concentration will effectively change a surface's thermal conductivity and wettability to meet the requirements of various applications.

Nanofluids play a vital role in heat transfer, solar energy, heat exchangers, the oil and gas industry, cooling technology, and thermal energy storage systems. Figure 1 explains the number of publications on nanofluids per year; the number represents the significance of the nanofluids for researchers. In Figure 2, the graph represents the publications of different fields, such as engineering, sciences, mathematics, etc. Figures 3 and 4 define the importance of nanofluid cavities for the different nanofluid applications.

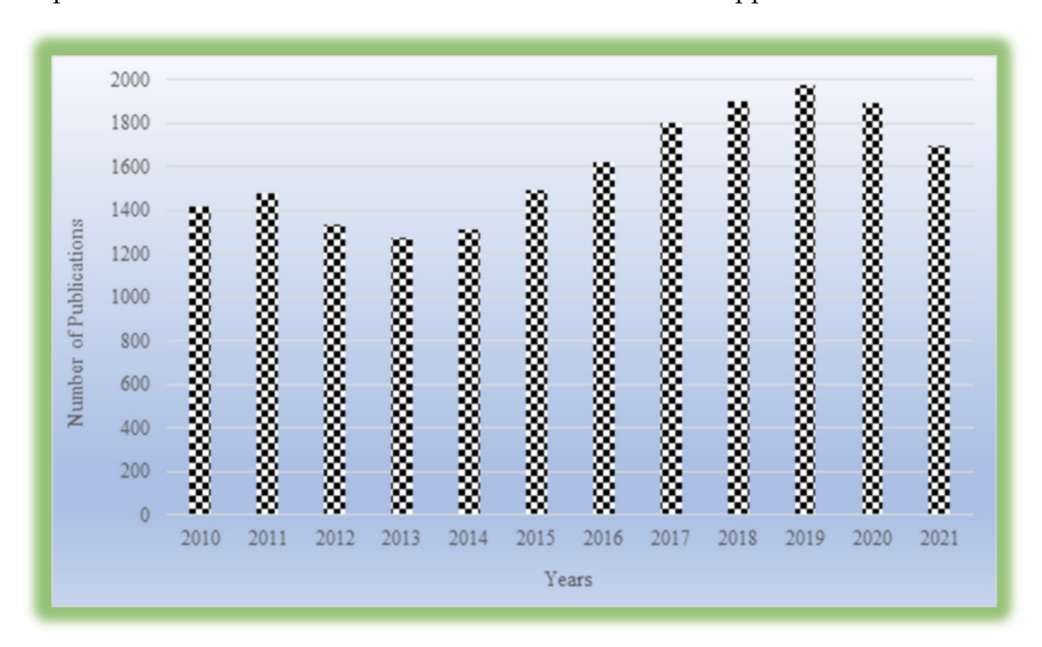


Figure 1. Number of publications published on nanofluids per year (1 January 2010–31 December 2021, search word nanofluid on Scopus.com).

Processes 2023, 11, 834 3 of 24

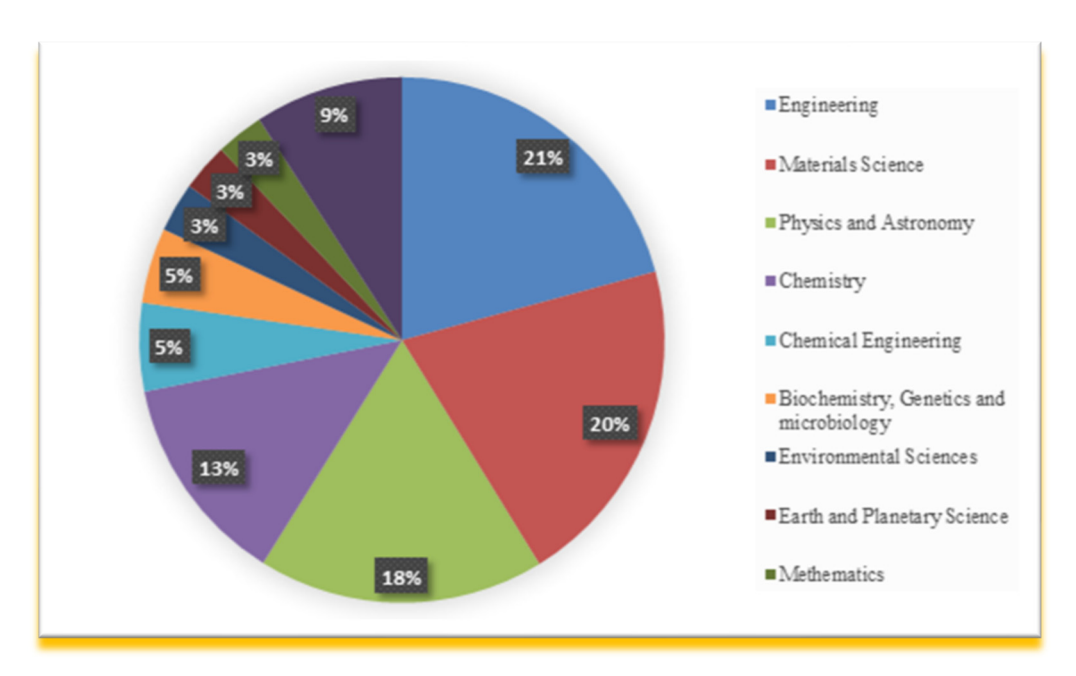


Figure 2. The Publications of nanofluids with respect to different fields of research (source: Scopus.com).

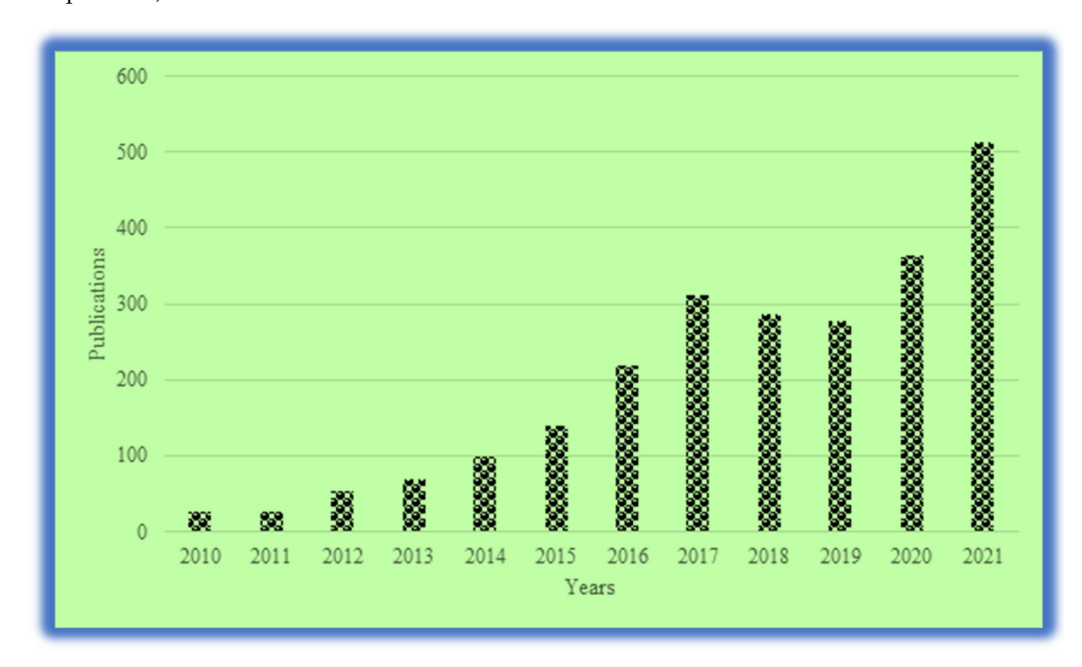


Figure 3. Area-wise contribution of publications on nanofluids published in different domains (source: Scopus.com).

Many engineering and industrial processes lead to the production of entropy, which consumes all the energy in the system. Knowing how quickly entropy is generated is critical to obtaining the most out of a system and using the least energy. When studying porous media, it is often vital to know the fields of temperature and velocity, as well as the pressure and other similar things. Other factors may also be relevant [3–8]. This is because the second rule of thermodynamics applies to all reversible flow and heat transfer processes. The reason for this is the fact that heat cannot be created or destroyed. Yet, the second law of thermodynamics is not often used to study the entropy. Heat transfer has demonstrated over the past three decades that the second law of thermodynamics must be applied when making thermal design decisions for porous media. The researchers believe that this new technology has a good chance of improving the design of thermal systems.

Processes 2023, 11, 834 4 of 24

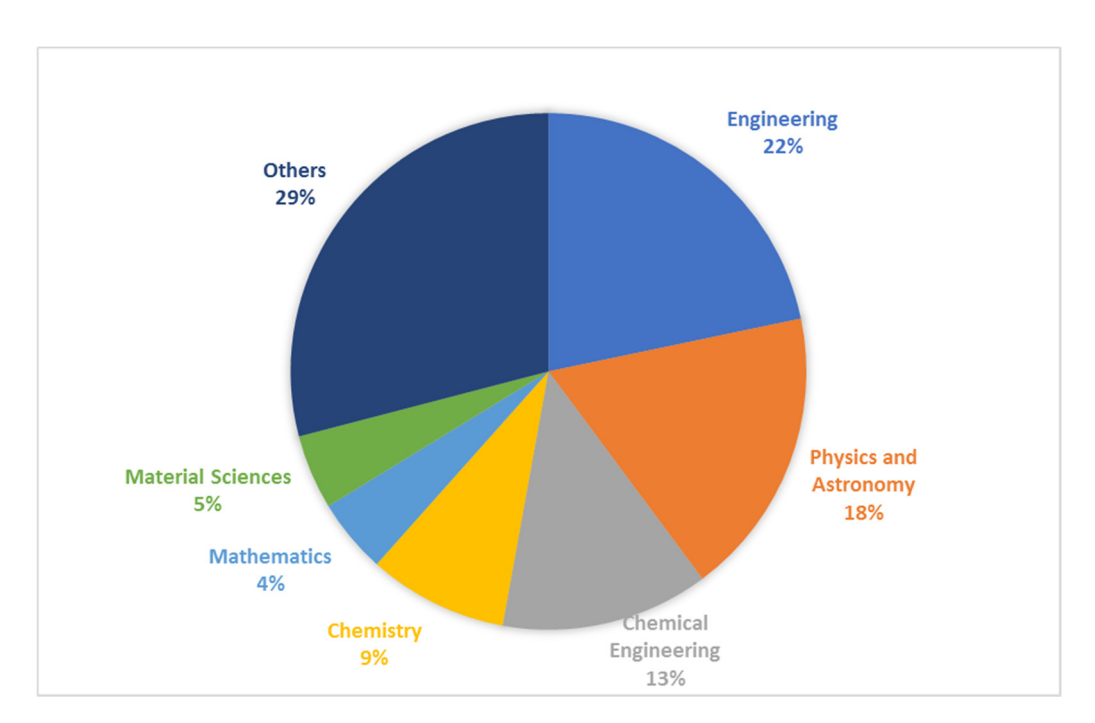


Figure 4. Publications on nanofluids using cavities in different disciplines.

The review focuses on the following points, which are shown in Figure 5.

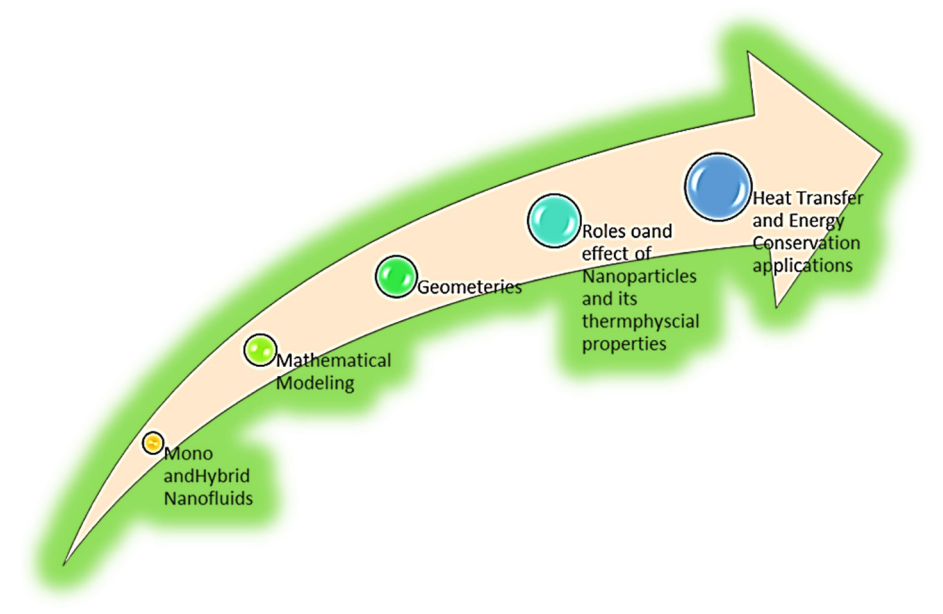


Figure 5. The flow of the review.

2. Literature Review

Many heat transfer engineering applications rely on the basic features of fluid flows and their importance in cavities. Oil extraction in grooved wet clutches, thermal energy storage, solar collectors, and heat exchange thermal performance augmentation are examples of such uses [9]. The examples include building cooling systems, food drying, heat exchangers, and nuclear reactors [10]. In recent years, many writers have examined natural, forced, and changing convection in the hollows of various geometries. The shape of lid-driven cavities is accessible in various structures and geometries in engineering applications, including square, rectangle, triangle, and trapezoidal, as well as other designs with a wide range of thermal boundary settings. Table 1 summarizes the information and relevance of the

Processes 2023, 11, 834 5 of 24

cavities, the various nanoparticles, and the various heat transfer phenomena investigations in various fluids.

Table 1. Nanoparticles and cavities studies in convective heat transfer.

Ref.	Type of Fluid	Cavities	Nanoparticles	Mechanism	Remarks
[11]	Nanofluid, viscous fluid	Square	Cu-water	Free convection	When thermal conductivity decreases, the heat transfer rate also decreases inside the cavity.
[12]	Nanofluid, viscous fluid	Square	Cu, Ag	Natural convection	Copper nanoparticles exhibit the highest heat transfer rates, whereas Ag nanoparticles exhibit the lowest.
[13]	Nanofluid, MHD	Wavy wall cavity	-	Natural convection	Increase in Hartmann number, decrease in heat transfer.
[14]	Non-Newtonian nanofluid	Porous square cavity	Cu	Natural convection	The rate of heat transmission as well as the various irreversibilities all improve with a higher Rayleigh number.
[15]	Nanofluid, viscous fluid	Triangular	-	Free convection	As Rayleigh and Lewis values drop, average Nusselt rises.
[16]	Ferrofluid	Trapezoidal	Fe ₃ O ₄	Natural convection	The inclination angle = $\pi/2$, demonstrating the instabilities inherent in heat and fluid flow.
[17]	Nanofluid, viscous fluid	Lid-driven cavity	CuO	Mixed convection	Adding nanoparticles is more valuable for improving local heat transfer.
[18]	Nanofluid, viscous fluid	Inclined wavy	CuO	MHD, Natural convection	Increases in the number of undulations result in a decrease in convective flow and an increase in heat transfer.
[19]	Nanofluid, viscous fluid	Porous undulant wall cavity	-	Natural convection	As heater temperature rises, fluid Nusselt number drops. Local Nusselt number increases when the cylinder is raised.
[20]	Nanofluid, viscous fluid	Open porous cavity	CuO	MHD, Free convection	As Darcy and Raleigh values increase, so does the rate at which warmer fluid leaves.
[21]	Nanofluid, viscous fluid	Rectangular cavity	CuO	MHD, Free convection	Angle of inclination of the magnetic field increases; the average Nusselt number decreases as the Hartmann number rises.
[22]	Nanofluid, viscous fluid	Porous cavity	CuO	Natural convection	The best heat transmission performance for high and low Ra values can be seen in cases D (hot and cold points are located at the top of the cavity) and C (hot and freezing points are located at the top and bottom of the hot and cold walls, respectively).
[23]	Nanofluid, viscous fluid	Lid-driven cubic cavity	Al_2O_3	MHD, Forced convection	A magnetic field enhances the heat transfer rate.
[24]	Nanofluid, viscous fluid	Porous cavity	Al ₂ O ₃ -H ₂ O	Forced convection	Temperature gradients are proportional to Darcy and Reynolds numbers. Increased Lorentz forces result in a decrease in the Nusselt number.
[25]	Nanofluid,	Porous cavity	Cu-H ₂ O	MHD, Forced convection	The results reveal that using nanoparticles with a platelet form results in the highest heat transmission rate. Nusselt number increases with the Darcy and Reynolds numbers but drops as the Lorentz force increases.
[26]	Nanofluid, viscous fluid	Porous corrugated cavity, rectangular shape cavity	-	MHD	The heat transmission rate increases as the Rayleigh number and wavelength parameter are raised. The Darcy and Hartmann numbers have no discernible influence on the temperature distribution.

Processes 2023, 11, 834 6 of 24

 Table 1. Cont.

Ref.	Type of Fluid	Cavities	Nanoparticles	Mechanism	Remarks
[27]	Micropolar nanofluid, viscous fluid	Square	CuO	Conjugate natural convection	As the porosity advances in response to the low pass, traditional Naiver–Stokes equations govern the flow of the nanofluids.
[28]	Nanofluid, viscous fluid	Square	CuO, Al ₂ O ₃ , Ti ₂ O	Natural convection	An increase in heat transfer compared to the base fluid (water) has been seen for all Rayleigh number ranges (Ra). For the purpose of describing heat transfer rates and temperature patterns created utilizing heat lines, the presence of viscous or buoyant forces is critical.
[29]	Non-viscous fluid	Spherical cavity	-	Thermodynamically coupled heat and water flow	A significant rise in pore pressure and displacements due to the existence of thermodynamically connected flows, but does not affect temperature.
[30]	Nanofluid, viscous fluid	Square	CuO	Natural convection	The sole use of nanofluid in a transparent cavity demonstrated that raising the nanofluid volume fraction increases Nu for $Ra = 10^3$, while there is an ideal concentration for different Ra values to optimize the average Nu .
[31]	Non-Newtonian nanofluid, viscous fluid	Porous cavity	-	Natural convection	Increasing the Lewis number boosts the overall irreversibility. Moreover, as the number of buoyancy ratios increases, the overall generation of entropy increases.
[32]	Ferrofluid	Square cavity	Cobalt	Natural convection	The increase in the Hartman number negatively impacts isotherms and streamlines circulations.
[33]	Ferrofluid	Linearly heated cavity	Kerosene and cobalt	Natural convection	Heat transport declines with increasing volume percentage of ferromagnetic particles at the nanoscale for different Rayleigh numbers.
[34]	Viscous fluid	Square cavity	-	Natural convection	Nonuniform heating of the bottom wall causes a faster rate of heat transfer to the centre of the bottom wall than uniform heating does for all Rayleigh numbers.
[35]	Newtonian fluid, viscous fluid	Inclined cavity	-	Natural convection	Calculating maps of local entropy generation is possible and can provide vital information for choosing an appropriate inclination angle.
[36]	Nanofluid, viscous fluid	Nanofluid-filled cavity	Cu	MHD, Natural convection	Heat transport decreases when the Hartmann number rises for various Rayleigh numbers.
[37]	Nanofluid, viscous fluid	Porous wavy wall cavity	-	Natural convection	The rate of heat transmission dramatically increases as dispersion increases.
[38]	Nanofluid, viscous fluid	Square porous cavity	-	Natural convection	According to the findings, increasing the viscosity change parameter enhances convective flow and heat transmission in a porous medium but has the opposite effect in pure fluids.
[39]	Viscous fluid, nanofluid	Square porous cavity	-	Natural convection	The thermophoresis, buoyancy ratio, and phase deviation are progressive functions of the Nusselt and Sherwood values. Additionally, this includes the Lewis number, Brownian motion, and amplitude ratio's decrementing functions.
[40]	Viscous fluid, nanofluid	Square cavity	Cu-water	MHD, Natural convection	Heat transfer and flow have no effect on the direction of a slip wall when slip parameters are present.

Processes 2023, 11, 834 7 of 24

Table 1. Cont.

Ref.	Type of Fluid	Cavities	Nanoparticles	Mechanism	Remarks	
[41]	Viscous nanofluid	Square cavity	-	Free convection	Heat transfer and flow have no effect on the direction of a slip wall in the presence of slip parameters.	
[42]	Viscous nanofluid	Lid-driven cavity	Cu-water	Mixed convection	Heat transfer could be improved by up to 8.3% with the improved heterogeneous porous medium.	
[43]	Incompressible viscous, nanofluid	Square cavity	-	Natural convection	The effect of thermophoresis results in a low concentration of nanoparticles near the porous wall's hot vertical interface. However, there is a high concentration near the cold vertical interface.	
[44]	Viscous nanofluid	Square cavity	Al ₂ O ₃ water	MHD, Mixed convection	With a constant Richardson number, the maximum stream function value increases when the porosity parameter and the Darcy number are increased.	
[45]	Nanofluid flow	Rectangular cavity	CuO	Natural convection	The rate of heat transfer increases as the number of grooves on the inner rods increases.	
[46]	Viscous nanofluid	Porous cavity	-	Mixed convection	Heat transfer is enhanced when the number of petals is even, as opposed to odd.	
[47]	Non-Newtonian nanofluid	Rectangular cavities	Fe ₃ O ₄ , CuO, and Al ₂ O ₃	MHD, Thermal analysis, entropy generation	The geometric parameters increase the local and average Nusselt numbers, as do the various entropy generation terms.	
[48]	Ferrofluid	Porous cavity	Fe ₃ O ₄ -H ₂ O	Natural convection	The magnetic field is an excellent heat transfer controller.	
[49]	Nanofluids	Square cavity	Cu	Natural convection	Cu provides maximum heat transfer.	
[50]	Nanofluid, incompressible	Square vented cavity	-	Mixed convection	Changes in porosity have a more significant influence on heat transfer with lower Richardson values. This results in an increase of around 79 percent in the Nusselt number in the best condition at conductivity ratios of 33.33 (Ri = 0.1) and 17.4 percent in the worst situation at conductivity ratios of 10 (Ri = 10).	

Closed cavity flow and heat transfer problems are more complex than open channel flow and heat transfer problems. Many challenges must be overcome, including geometry and boundary conditions, the type of governing equations used, and the finding of the optimal numerical solution. A large amount of literature may cover these critical physical difficulties. This crucial research topic has risen to prominence due to its unavoidable applications. Examples include home heating and cooling, microprocessors, air conditioning, solar collectors, and other related uses. The researchers have always worked to improve the performance of such procedures to increase their efficiency.

Many researchers have conducted experimental and mathematical experiments, the results of which have been published. Due to the low thermal conductivity of conventional heat transfer fluids such as water, oil, and ethylene glycol, the use of mono and hybrid nanofluids can provide a higher heat transfer rate. It is the most significant impediment to improving the performance and compactness of many electrical engineering devices. The Rayleigh number is an important parameter regulating heat transmission in porous media. The researchers investigated how the Rayleigh number, the nanoparticles' solid volume fraction parameter, the porosity of the porous medium, the porous medium, and the factual matrix of the porous medium affect the flow field, temperature distribution, and the Nusselt number [51–53].

Inside the cavity, regardless of the Rayleigh number or the material used to create the solid porous medium matrix, only one circular circulation flow occurs. The flow cell elongates along the horizontal axis as the Rayleigh number increases, and the boundary Processes 2023, 11, 834 8 of 24

layers thicken. It strengthens conventional flow. The increase in Rayleigh numbers for the glass beads used as the porous medium's solid matrix results in a decrease in the porosity range where the heat transmission by convection is low [9–15].

Modern metallurgy and metalworking are fascinated by the MHD flow and heat transmission of electrically conductive fluid because it transfers a considerable quantity of energy. In numerous technical applications, such as MHD generators, plasma research, nuclear reactors, fuel from geothermal sources, and metal from non-metallic enclosures, MHD generators are researched.

As the Hartmann number (Ha) grows, heat conduction becomes the predominant mechanism of energy transfer, followed by commensurate declines in the heat transfer rate, ferrofluid rate, and entropy creation rate. The best values for the magnetic field tilt angle and intensity selection vary with the engineering application, even if the oscillation phases for the mean Nusselt number and average entropy generation are the same. When the porous layer is kept thick, heat transport will be slowed, and entropy will increase.

MEMs, coating and solidification, food processing, and nuclear reactor cooling are all important geotechnical engineering applications for lid-driven cavities. The interaction between shear-driven flow and buoyancy is quite complex, and it has a significant impact on how efficiently flow mixes and heat are transferred. Using numerical simulations for various flow parameters, it is possible to simulate mixed convection and entropy generation in nanofluid-filled lidded cavities under the influence of inclined magnetic fields imposed on their upper and lower triangular domains. The effect of the magnetic tilt angle was found to be more pronounced for common values of the Richardson number (Ri) and negligible for high values of Ri. Entropy generation decreases as the Ra value increases. Due to the high temperature gradients along the bottom, the effect is more prominent in the lower triangular area. Entropy production declines as the solid volume fraction increases. As the Ha grows, the suppression of fluid motion inside the cavity for the bottom and upper triangular domains reduces the total development of entropy [13–15]. The researchers also work on different non-Newtonian nanofluid models to find out the maximum heat transfer rate [31,54].

In most engineering applications, the system boundaries can take a curved shape. This technology is used to build robots, toys, spacecraft, and other electrical gadgets. The irregularity of the grid at the boundary points makes it more difficult to solve these geometries using computing than it is to solve problems involving the solution of regular shapes such as squares, circles, or rectangles. In these kinds of situations, cavities can be heated by one or two walls running the length of the wall, a full-wall partial heater, or both. It is common practice in the design of electronic devices for nanofluid or neat fluid-filled chambers to include either a partially or a completely recessed heating source. It has been said that the higher the Hartmann number, the less the convection flow and heat transfer rate, but the overall generation of entropy increases [55,56]. As a result of the fact that the radiation parameter can be either an increasing or a decreasing function of the Darcy number, it influences the transmission of heat and the flow of fluid. As a result of the fact that the heater and the cooler are in separate locations, the angle of inclination of the cavity shifts quite a bit, which has a significant impact on the flow of fluid and the temperature. The influence of the magnetic field also has the additional effect of decreasing the heat transmission rate inside the cavity. This is true because when the magnetic field is applied in the horizontal direction, pure conduction becomes the primary mode of operation [56]. Free convection and conduction mechanisms are responsible for most of the heat transfer. When added to the base fluid, nanoparticles have the potential to raise the viscosity of the nanofluid while simultaneously enhancing the thermal conductivity of the nanofluid, which has the effect of reducing the strength of the convective flow field. A similar thing can occur when a porous layer is applied; the rate of heat transfer by conduction will increase, while the rate of heat transfer via free convection will decrease.

Entropy generation has garnered significant attention owing to its reputation in numerous natural and industrial applications. For example, studying the rate at which entropy

Processes 2023, 11, 834 9 of 24

is created is essential in engineering because it helps them figure out the irreversibility of thermodynamics more accurately [57–60].

In the past two decades, much of the research has focused on convective heat and mass transfer through porous media. Numerous engineering applications involving forced and free convection in permeable channels and cavities with simple and complex geometries, such as rectangular cavities and cylindrical containers, have been studied using various numerical, experimental, and analytical techniques.

The entropy generation function quantifies the level of irreversibilities accessible in a process. When irreversibilities are present, the performance of the engineering equipment decreases, and the entropy generation function is used to determine this level. As the development of entropy is the criterion for measuring the available work destruction of systems, minimizing the effect of entropy is crucial to achieving the optimal design of energy systems [61].

Additionally, entropy formation causes systems to either decrease usable power cycle outputs, as with devices that produce power or increase power input and as with devices that consume energy [62], which is why the second law is more reliable.

3. Significance of The Review

Nanofluids offer an extensive array of applications in engineering challenges, as they do in aerodynamics, nuclear reactors, heat exchangers, etc. They produce impressive results that entice researchers to employ them for various applications. Several reviews [62–66] on nanofluids help researchers and scientists to gain more knowledge and to apply it to different industrial problems to solve them and obtain convincing results. Still, according to a thorough literature review, the appropriate mathematical models play a critical role in enhancing heat transfer, saving energy, and lowering production costs in various realworld applications. However, there are very few reviews. Much research is currently being conducted in the literature on the use of cavities in nanofluid flow in convective heat transfer [10,67–69]. We prepared a review of the mathematical models and the use of cavities in nanofluid flow for convective heat transfer and entropy generation, which are giving efficient results in different applications such as thermal energy storage systems, cooling technology, and temperature control systems in buildings and infrastructure.

4. Mathematical Modeling

In nanofluid flow, different mathematical models are employed to predict how the flow will behave to improve heat transfer by using different shapes and cavities. The two-phase nanofluid model of Buongiorno [70], the nanofluid model of Tiwari and Das, the Brinkmann model, and the Darcy–Forchheimer Extended Brinkmann model [71] are well-known models. According to the literature, the model of Tiwari and Das is very efficient for a uniform flow of nanofluids; thus, we delve deeper into the Tiwari and Das model in this review; however, the study on this model has not been published.

4.1. Tiwari and Das Nanofluid Model

Tiwari and Das [72] created a mathematical model of a single-phase nanofluid to study nanofluid behavior in a square cavity driven by a differentially two-sided cavity. Three distinct situations were considered, as seen in Figure 6. The left (cold) wall rises in this scenario, whereas the right (hot) wall flowers. In cases II and III, the left wall descends, the right wall ascends, and both walls ascend simultaneously. In all three scenarios, the moving walls travel at the same speed, and the gravitational force is parallel. The following steps of the fluid flow were observed:

Processes 2023, 11, 834 10 of 24

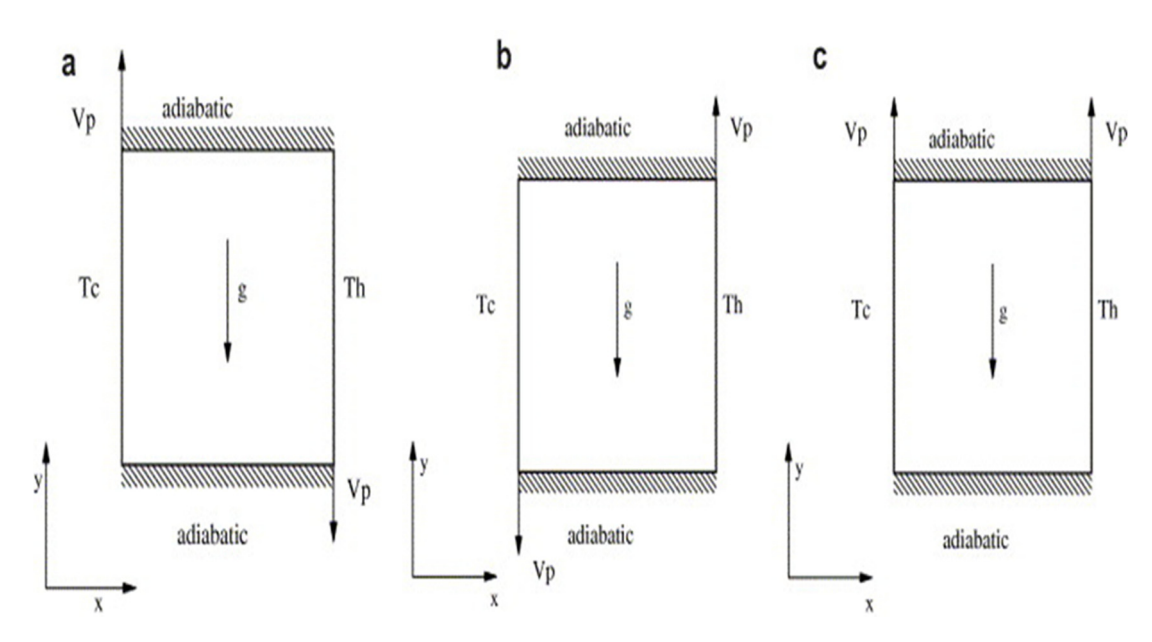


Figure 6. The geometry of the Tiwari and Das model (a) case 1, (b) case 2 and (c) case 3 [72].

In Figure 6, V_p defines the velocity of the moving liquid, where T_c and T_h represent the temperatures at the hot and cold walls of the cavity and g is gravity. In Figure 6, a, b, and c represent the three different cases of temperature distribution in heat transfer in the cavity. The mathematical model is composed of the following equations:

$$\frac{\partial u^{-}}{\partial x^{-}} + \frac{\partial v^{-}}{\partial y^{-}} = 0 \tag{1}$$

$$\frac{\partial u^{-}}{\partial t} + \frac{\partial u^{-2}}{\partial x^{-}} + \frac{\partial u^{-}.v^{-}}{\partial y^{-}} = -\frac{1}{\rho_{nf,0}} \frac{\partial p}{\partial x^{-}} + \frac{\mu_{eff}}{\rho_{nf,0}} \left(\frac{\partial^{2} u^{-}}{\partial x^{-2}} + \frac{\partial^{2} u^{-}}{\partial y^{-2}} \right)$$
(2)

$$a \frac{\partial v^{-}}{\partial t} + \frac{\partial u^{-}.v^{-}}{\partial x^{-}} + \frac{\partial v^{-2}}{\partial y^{-}} = -\frac{1}{\rho_{nf,0}} \frac{\partial p}{\partial y^{-}} + \frac{\mu_{eff}}{\rho_{nf,0}} \left(\frac{\partial^{2}v^{-}}{\partial x^{-2}} + \frac{\partial^{2}v^{-}}{\partial y^{-2}} \right) + \frac{1}{\rho_{nf,0}} (\varphi \rho_{s,0} \beta_{s} + (1 - \varphi)\rho_{f,0}\beta_{f} (T - T_{C})),$$
(3)

$$\frac{\partial T}{\partial t} + \frac{\partial u^{-}.T}{\partial x^{-}} + \frac{\partial v^{-}.T}{\partial y^{-}} = \alpha_{nf} \left(\frac{\partial^{2} T}{\partial x^{-2}} + \frac{\partial^{2} T}{\partial y^{-2}} \right)$$
(4)

$$\alpha_{nf} = \frac{k_{eff}}{(\rho C_P)_{nf,0}},\tag{5}$$

where u^- , v^- are the x^- and y^- components of the velocities, respectively, and x^- , y^- are the horizontal and vertical components, respectively, of the cavity. The physical parameters of the nanofluids employed in this model to solve the problem are summarized in Table 2.

Table 2. Thermophysical properties employed in the Tiwari and Das model.

Effective Viscosity	$\mu_{eff} = \frac{\mu_f}{(1-\varphi)^{2.5}}$	
Effect of density at reference temperature	$\rho_{nf,0} = (1-\varphi)\rho_{f,0} + \varphi\rho_{s,0}$	
Heat capacitance	$(\rho C_P)_{nf} = (1 - \varphi)(\rho C_P)_f + \varphi(\rho C_P)_s$	
Thermal conductivity	$rac{k_{eff}}{k_{f}} = rac{(k_{s} + 2k_{f}) - 2\varphi(k_{f} - k_{s})}{(k_{s} + 2k_{f}) + \varphi(k_{f} - k_{s})}$	
Thermal conductivity enhancement coefficient	$K = \frac{k_{eff} - k_f}{k_{HC} - k_f}$	

The Tiwari and Das models are some of the most attractive models for modeling Newtonian fluids (nanofluids) among researchers. This model's capacity to replicate a

Processes 2023, 11, 834 11 of 24

wide range of Newtonian nanofluids is one reason for its appeal. Table 3 summarizes some of the studies conducted on Newtonian fluids in cavities. These investigations used the Tiwari and Das models to determine fluid flow in cavities.

4.2. Role of The Entropy Generation in Cavities

Improving heat transfer efficiency in areas such as electronic cooling, heat exchangers, and food drying is one of the most complex engineering challenges. In certain industrial applications, the dispersion of solid nanoparticles with high thermal conductivity in a pure fluid to increase the heat transfer rate has recently gained popularity. For example, one of the fluid-based coolant alternatives for cooling electronic chips and processors with high cooling requirements is this fluid-based coolant, which incorporates nanoparticles suspended in pure liquid [73].

The researchers study entropy generation using square, U-shaped, triangular, and wavy cavities, copper and aluminium nanoparticles, and the Tiwari and Das nanofluid mathematical model [58,73–77]. The experts have also researched how nanofluids move heat through cavities driven by lids using mixed convection. In a variety of industrial system preferences, mixed convective flow and heat transfer in cavities can be performed, including ingot solidification, float glass processing, coating or continuous reheat furnaces, and any other place where a solid material or heat moves from one chamber to another, because the wall moves and the temperature changes, shear force, and buoyancy force all play a role in how heat moves.

Adding nanoparticles reduces the buoyancy effects for the current range of parameter values, and the forced convection heat transfer mechanism takes over as the dominant heat transfer mechanism. It is possible to achieve much more heat transfer than entropy generation in a nanofluid at high Grashof numbers. This is true for many Reynolds and Grashof numbers [74,75]. In a corrugated cavity, increasing the Raleigh number intensifies the convective flow and heat transfer. In contrast, increased fluid friction causes a decrease in the average Bejan number. A convective plume forms above the upper wavy ridge as the Ra increases, as do the non-monotonic changes in the mean Nusselt and Bejan numbers over time. The primary convective flow inside the cavity becomes more intense as the number of ripples increases, and the domain of interest cools more rapidly. The effects of increasing the number of ripples are as follows: as *k* increases, the heat transfer rate and average entropy generation due to heat transfer decrease, lowering all the critical parameters considered [77]. To better understand heat transfer and entropy generation in a cavity with sinusoidal roughness elements on the bottom wall, the researchers [76] used numerical simulation. Following careful examination, the results show that entropy generation due to heat transfer contributes significantly to the increase in total entropy generation. At low Ra and low Re, the entropy generation could be kept to a bare minimum at a constant N and A, where A is the amplitude of the roughness surface on the cavity's surface. Adding a minor feature to a heated surface could be an excellent alternative to smooth surfaces to reduce entropy and increase the amount of heat that can be transferred.

The generation of entropy in a nanofluid under LTNE for different positions of the heated wall of the enclosure has been studied using the nanofluid models of Tiwari and Das. This research is beneficial in improving system performance while simultaneously reducing entropy generation. The irreversibility of the system is significantly controlled by buoyancy and magnetic forces, with the angle of inclination of the magnetic field having only a marginal effect. When the heated wall is located in the upper part or vertical wall of the envelope, the geometry of the angle of inclination affects the irreversibility. However, this does not change the irreversibility of the two heated wall positions on the other side [78].

Finally, it is possible to improve or optimize the thermodynamic performance of engineering systems by employing strategies such as entropy generation analysis and minimization, which are both effective approaches. The development of these approaches spans multiple decades and has resulted in the creation of design processes, the evolution of which has been driven primarily by the assistance of computer resources. Entropy

Processes 2023, 11, 834 12 of 24

generation analysis is harder to use with non-steady processes because you have to look for an optimal time history, which means minimizing the amount of entropy made in a finite amount of time. Because of this, entropy generation is rarely used to deal with transient operations and conditions that are not what was planned. This is a big gap in the research because most of the energy systems that people are interested in right now, such as energy storage, solar systems, and micro-cogeneration, work under unsteady state protocols or are affected by natural changes in the time of the primary energy inflow.

4.3. Impact of the Correlations of Thermal Conductivity in Cavities

The researchers are trying out different cavities in nanofluid flows to see which ones allow heat to move the fastest. In this section's middle part, we will talk briefly about the extension of the Tiwari and Das single-phase nanofluid mathematical model and the extension of different correlations in the physical properties of nanoparticles, such as the thermal conductivity, specific heat capacity, and viscosity correlation of nanofluids in cavities and how they affect heat transfer. Tables 3 and 4 provide the details of the thermophysical properties used in different geometries with the Tiwari and Das model.

Table 3. Different thermal conductivity correlations used by researchers using the Tiwari and Das model for various geometries.

Ref.	Cavity/Geometry	N. P	Thermal Conductivity	Remarks
[79]	Square	Ag	$k_{nf} = k_f \left(\frac{k_p + 2k_f - 2\varphi(k_f - k_p)}{k_p + 2k_f + 2\varphi(k_f - k_p)} \right)$	Heat transfer rate increases in the range of 6.3–12.4% at $\varphi_o = 0.05$.
[80]	Chamber	Al_2O_3	$k_{nf} = k_f \left(1 + 2.944 \varphi + 19.672 \varphi^2 \right)$	Heat flow rate increases with nanoparticle concentration for high Rayleigh numbers.
[11]	Porous square cavity	Cu	$k_{mnf} = k_m \left(1 - \frac{3\epsilon \varphi \left(k_f - k_p \right)}{k_m \left(k_p + 2k_f + \varphi \left(k_f - k_p \right) \right)} \right)$	Less conductivity of the solid material reduces convective heat transport within the cavity.
[81]	Porous parabolic cavity	Cu, Al ₂ O ₃	$k_{mnf} = k_m \left(1 - \frac{3\varepsilon\varphi(k_f - k_p)}{k_m(k_p + 2k_f + \varphi(k_f - k_p))} \right)$	Reduction in the porosity upsurge of the thermal conductivity of the porous matrix, whereas decreased inclination angle and aspect ratio exacerbate the heat transfer degradation.
[82]	Triangular cavity	Cu, CuO, Al ₂ O ₃ , TiO ₂	$k_{nf} = k_f \left(\frac{k_s + 2k_f - 2\varphi(k_f - k_s)}{k_s + 2k_f + \varphi(k_f - k_s)} \right)$	For all Rayleigh numbers, increases the nanoparticle volume in pure water and increases the rate of change in the heat transfer rate.
[83]	Square porous cavity	Cu, Aluminum foam	$k_{mnf} = k_m \left(1 - \frac{3\varepsilon \varphi(k_f - k_p)}{k_m(k_p + 2k_f + \varphi(k_f - k_p))} \right)$	Thermal stratification has a critical effect on heat and fluid flow fields.
[84]	Moving needle	Al ₂ O ₃	$k_{nf} = k_f \left(1 + 2.944 \varphi + 19.672 \varphi^2 \right)$	While the combined action of Dufour and Soret diffusions increases the heat transfer coefficient, the mass transfer coefficient shows a dual behavior.
[85]	Triangular cavity	Al_2O_3	$k_{nf} = k_f \left(\frac{k_p + 2k_f - 2\varphi(k_f - k_p)}{k_p + 2k_f + \varphi(k_f - k_p)} \right)$	At Ri = 100, the average heat transfer enhances to $48.26\%.$
[86]	Wavy wall cavity	-	$k_{nf} = k_f \left(1 + 2.944 \varphi + 19.672 \varphi^2 \right)$	The average Nusselt number decreases with the increasing nanoparticle volume fraction for all inclination angles except = $\pi/4$, where nanoparticles improve heat transmission.
[87]	Shrinking sheet	TiO ₂ , Al ₂ O ₃ , Cu	$k_{nf} = k_f \left(\frac{k_s + 2k_f - 2\varphi(k_f - k_s)}{k_s + 2k_f + \varphi(k_f - k_s)} \right)$	The addition of suction and sliding results expands the range of existing dual solutions.
[88]	Shrinking sheet	TiO ₂ , Al ₂ O ₃ , Cu	$k_{nf} = k_f \left(\frac{k_s + 2k_f - 2\varphi(k_f - k_s)}{k_s + 2k_f + \varphi(k_f - k_s)} \right)$	The skin friction coefficient and the local Nusselt number at the sheet's surface upsurge as the suction rate increases.
[89]	Rotating disk	Fe ₃ O ₄	$k_{nf} = k_f \left(\frac{k_s + 2k_f - 2\varphi(k_f - k_s)}{k_s + 2k_f + \varphi(k_f - k_s)} \right)$	The addition of ferromagnetic particles improves the convective heat transfer coefficient of water.
[90]	Porous cylinder	Au-Ag H2O	$\big[\frac{^{k_{s2}+2k_{nf}-2\varphi_{2}\left(k_{nf}-k_{s2}\right)k_{s1}+2k_{f}-2\varphi_{1}\left(k_{f}-k_{s1}\right)}}{k_{s2}+2k_{nf}+\varphi_{2}\left(k_{nf}-k_{s2}\right)k_{s1}+2k_{f}+\varphi_{1}\left(k_{f}-k_{s1}\right)} \big] k_{f}$	Hybrid nanofluids may be recommended for heat transfer applications to improve the thermophysical properties of conventional fluids and mono nanofluids.
[91]	Sheet	Cu, Al ₂ O ₃	$k_{nf} = k_f \left(\frac{k_s + 2k_f - 2\varphi(k_f - k_s)}{k_s + 2k_f + \varphi(k_f - k_s)} \right)$	Cu gives best performance as compared to $\mathrm{Al}_2\mathrm{O}_3$.

Processes 2023, 11, 834 13 of 24

Table 3. Cont.

Ref.	Cavity/Geometry	N. P	Thermal Conductivity	Remarks
[92]	Sheet	Cu, Al ₂ O ₃	$k_{nf} = k_f \left(\frac{k_s + 2k_f - 2\varphi(k_f - k_s)}{k_s + 2k_f + \varphi(k_f - k_s)} \right)$	Cu gives maximum heat transfer rate.
[93]	Vertical cone	TiO ₂ , Al ₂ O ₃ , Cu	$k_{nf} = k_f \left(\frac{k_s + 2k_f - 2\varphi\left(k_f - k_s\right)}{k_s + 2k_f + \varphi\left(k_f - k_s\right)} \right)$	The size of the nanoparticle is significant in heat transfer enhancement.
[94]	Cone	Cu, Al ₂ O ₃	$k_{nf} = k_f \left(\frac{k_s + 2k_f - 2\varphi(k_f - k_s)}{k_s + 2k_f + \varphi(k_f - k_s)} \right)$	Alumina and copper nanoparticles have the lowest and highest values of the skin friction coefficient.
[95]	Circular cylinder	TiO ₂ , Al ₂ O ₃ , Cu	$k_{nf} = k_f \left(\frac{k_s + 2k_f - 2\varphi(k_f - k_s)}{k_s + 2k_f + \varphi(k_f - k_s)} \right)$	Cu gives maximum heat transfer.
[96]	Shrinking sheet	TiO ₂ , Al ₂ O ₃ , Cu	$k_{nf} = k_f \left(\frac{k_s + 2k_f - 2\varphi(k_f - k_s)}{k_s + 2k_f + \varphi(k_f - k_s)} \right)$	Cu gives maximum heat transfer.
[97]	Porous channel	Cu	$k_{nf} = k_f \left(\frac{k_s + 2k_f - 2\varphi(k_f - k_s)}{k_s + 2k_f + \varphi(k_f - k_s)} \right)$	The concentration increases considerably as the Schmidt number and chemical reaction parameter increase.

Table 4. Specific heat capacity and thermal diffusivity used by researchers using Tiwari and Das model in different cavities/geometries.

Ref.	Cavity	Nanoparticles	Specific Heat Capacity	Thermal Diffusivity
[79]	Square	Ag	$(\rho C_P)_{nf} = (1 - \varphi)(\rho C_P)_f + \varphi(\rho C_P)_P$	$\alpha_{nf} = \frac{k_{nf}}{\left(\rho C_P\right)_{nf}}$
[80]	Chamber	Al ₂ O ₃	$(\rho C_P)_{nf} = (1 - \varphi)(\rho c)_f + \varphi(\rho c)_P$	-
[11]	Porous square cavity	Cu	$(ho C_P)_{mnf} = [1 - \epsilon \varphi \frac{(ho C_P)_f - (ho C_P)_p}{(ho C_P)_m}] (ho C_P)_m$	$\alpha_{mnf} = \frac{k_{mnf}}{\left(\rho C_P\right)_{nf}}$
[81]	Porous parabolic cavity	Cu, Al ₂ O ₃	$(ho C_P)_{mnf} = [1 - \epsilon \varphi \frac{(ho C_P)_f - (ho C_P)_p}{(ho C_P)_m}]$	$\alpha_{mnf} = \frac{k_{mnf}}{\left(\rho C_P\right)_{nf}}$
[82]	Triangular cavity	Cu, CuO, Al ₂ O ₃ , TiO ₂	$(\rho C_P)_n = (1 - \varphi)(\rho C_P)_f + \varphi(\rho C_P)_s$	$\alpha_n = \frac{k_n}{(ho C_P)_n}$
[83]	Square porous cavity	Cu, Aluminum foam	$(\rho C_P)_{mnf} = (\rho C_P)_m [1 - \epsilon \varphi \frac{(\rho C_P)_f - (\rho C_P)_p}{(\rho C_P)_m}]$	$\alpha_{mnf} = \frac{k_{mnf}}{\left(\rho C_{P}\right)_{nf}}$
[84]	Moving needle	Al_2O_3	$(\rho C_P)_{nf} = (1 - \varphi)(\rho c)_f + \varphi(\rho c)_s$	-
[85]	Triangular cavity	Al_2O_3	$(\rho C_P)_{nf} = (1 - \varphi)(\rho c)_{bf} + \varphi(\rho c)_p$	-
[86]	Wavy wall cavity	-	$(\rho C)_{nf} = (1 - \varphi)(\rho c)_f + \varphi(\rho c)_p$	$\alpha_n = \frac{k_{nf}}{\left(\rho C_P\right)_{nf}}$
[87]	Shrinking sheet	TiO ₂ , Al ₂ O ₃ , Cu	$(\rho C_P)_{nf} = (1 - \varphi)(\rho c)_f + \varphi(\rho c)_s$	$\alpha_n = \frac{k_{nf}}{\left(\rho C_P\right)_{nf}}$
[88]	Shrinking sheet	TiO ₂ , Al ₂ O ₃ , Cu	$(\rho C_P)_{nf} = (1 - \varphi)(\rho c)_f + \varphi(\rho c)_s$	$\alpha_n = \frac{k_{nf}}{(ho C_P)_{nf}}$
[89]	Rotating disk	Fe ₃ O ₄	$(\rho C_P)_{nf} = (1 - \varphi)(\rho c)_f + \varphi(\rho c)_s$	-
[90]	Porous cylinder	Au-Ag water	$[(1-\varphi_{2})\;\{(1-\varphi_{1})\;(\rho C_{P})_{f}+\varphi_{1}(\rho C_{P})_{s1}\}s+\varphi_{2}\varphi_{1}(\rho C_{P})_{s2}$	$\alpha_n = \frac{k_{hnf}}{(\rho C_P)_{hnf}}$
[91]	Sheet	Cu, Al ₂ O ₃	$(\rho C)_{nf} = (1 - \varphi)(\rho c)_f + \varphi(\rho c)_p$	$\alpha_n = \frac{k_{nf}}{\left(\rho C_P\right)_{nf}}$
[92]	Vertical cone	TiO ₂ , Al ₂ O ₃ , Cu	$(\rho C_P)_{nf} = (1 - \varphi)(\rho c)_f + \varphi(\rho c)_s$	$\alpha_n = \frac{k_{nf}}{\left(\rho C_P\right)_{nf}}$
[93]	Cone	Cu, Al ₂ O ₃	$(\rho C_P)_{nf} = (1 - \varphi)(\rho c)_f + \varphi(\rho c)_s$	$\alpha_n = \frac{k_{nf}}{(\rho C_P)_{nf}}$
[94]	Circular cylinder	TiO ₂ , Al ₂ O ₃ , Cu	$(\rho C_P)_{nf} = (1 - \varphi)(\rho c)_f + \varphi(\rho c)_s$	$\alpha_n = \frac{k_{nf}}{(\rho C_P)_{nf}}$
[95]	Shrinking sheet	TiO ₂ , Al ₂ O ₃ , Cu	$(\rho C_P)_{nf} = (1 - \varphi)(\rho c)_f + \varphi(\rho c)_s$	$\alpha_n = \frac{k_{nf}}{\left(ho C_P\right)_{nf}}$
[96]	Porous channel	Cu	$(\rho C_P)_{nf} = (1 - \varphi)(\rho c)_f + \varphi(\rho c)_s$	$\alpha_n = \frac{k_{nf}}{\left(\rho C_P\right)_{nf}}$

Tables 3 and 4 list the different types of nanoparticles, geometries, and cavities and the correlations between the thermal conductivity, specific heat capacity, and viscosity that

Processes 2023, 11, 834 14 of 24

the researchers found in the nanofluids and hybrid nanofluids using the Tiwari and Das single-phase nanofluid model to obtain the most heat transfer.

Using nanofluids with different shapes and cavities is a better way to improve thermal performance than using each method separately. When researchers talk about nanofluids, they discuss fluids with nanoparticles in them [71,98,99]. Nanofluids are used for several reasons, the most important of which is that it is well known that they have better thermophysical properties, most notably higher thermal conductivity. Nanofluids are used for many different reasons, but the most important one is that it is well known that they have better thermophysical properties. The thermophoresis effect was caused by Brownian motion, which was caused by the increase in thermal conductivity [100–102]. Numerous pieces of research have reported on distinct cavities that contain a variety of nanofluids; these are described in Table 3.

The researchers have extended the Tiwari and Das model by incorporating different thermal conductivity correlations to achieve the greatest heat transfer rate possible using different nanoparticles in the nanofluid flow and various geometries. Most authors examine the thermal conductivity correlations and specific heat capacitance and viscosity with the Tiwari and Das model, as given in Equations (6)–(8):

$$k_{nf} = k_f \left(\frac{k_s + 2k_f - 2\varphi(k_f - k_s)}{k_s + 2k_f + \varphi(k_f - k_s)} \right),$$
 (6)

$$(\rho C_P)_{nf} = (1 - \varphi)(\rho c)_f + \varphi(\rho c)_s, \tag{7}$$

$$\mu_{nf} = \frac{\mu_f}{(1 - \varphi)^{2.5}},\tag{8}$$

In Equations (6) and (7), k_{nf} defines the thermal conductivity of the nanofluid; k_f represents the thermal conductivity of regular fluids; k_s defines the thermal conductivity of the solid, and φ defines the nanoparticle concentrations; ρ defines density; C_P explains the heat capacity; μ explains viscosity; and the subscripts f and nf represent the fluids and nanofluids. Chen [97] developed the mathematical model in the parameters of the dimensionless flux function and temperature, taking into account the Darcy–Boussinesq approximation and other factors.

The numerical analysis was carried out using the Tiwari and Das nanofluid model, which was updated to include more accurate empirical correlations for the physical parameters of the nanofluids. The author used the following correlation for thermal conductivity and specific heat capacity for the porous square cavity, as provided in Equations (9) and (10):

$$k_{mnf} = k_m \left(1 - \frac{3\varepsilon\varphi(k_f - k_p)}{k_m(k_p + 2k_f + \varphi(k_f - k_p))} \right)$$
(9)

$$(\rho C_P)_{mnf} = (\rho C_P)_m \left[1 - \epsilon \varphi \frac{(\rho C_P)_f - (\rho C_P)_p}{(\rho C_P)_m} \right]$$
(10)

where k_{mnf} represents the thermal conductivity of nanoparticles inserted in a porous medium; k_m represents the thermal conductivity of the porous medium; ε represents the porosity; φ represents the initial concentration of the nanoparticles; and the indices f and p represent the nanoparticles and clear fluid, respectively, and k_m represents the thermal conductivity of the porous medium. The use of copper nanoparticles in a porous square cavity results in a significant increase in heat transfer efficiency. The authors use aluminum foam and a glass bulb as porous media in the problem. The impact of copper nanoparticles in combination with aluminum as a porous medium increases the thermal conductivity, and as a result, the maximum heat transfer rate is attained.

Processes 2023, 11, 834 15 of 24

The researchers in [79,80,84,86] use the thermal conductivity correlation and specific heat capacitance in a nanofluid flow in a chamber, moving the needle and wavy wall cavity together with the Tiwari and Das model, as given in Equations (11) and (12):

$$k_{nf} = k_f \left(1 + 2.944 \varphi + 19.672 \varphi^2 \right) \tag{11}$$

$$(\rho C_P)_{nf} = (1 - \varphi)(\rho c)_f + \varphi(\rho c)_P \tag{12}$$

The above correlations also provide a maximum heat transfer rate. In hybrid nanofluids, the correlation of thermal conductivity and specific heat capacity is defined in Equations (13) and (14):

$$\frac{k_{s_2} + 2k_{nf} - 2\varphi_2(k_{nf} - k_{s_2})k_{s_1} + 2k_f - 2\varphi_1(k_f - k_{s_1})}{k_{s_2} + 2k_{nf} + \varphi_2(k_{nf} - k_{s_2})k_{s_1} + 2k_f + \varphi_1(k_f - k_{s_1})}$$
(13)

$$(1 - \varphi_2) \left\{ (1 - \varphi_1)(\rho C_P)_f + \varphi_1(\rho C_P)_{s_1} \right\} + \varphi_2 \varphi_1(\rho C_P)_{s_1}$$
(14)

In Equations (13) and (14), s_1 and s_2 define the solid particles of hybrid nanofluids. When it comes to improving heat transfer, the thermal conductivity and viscosity of the fluids play a significant role in the final product. It has been discovered that the utilization of hybrid nanofluids can boost the thermal conductivity of nanoparticles, which ultimately results in the highest possible rate of heat transmission.

The thermal conductivity of nanofluids is known to be superior to that of base fluids, as has been observed by the vast majority of the authors. The greater the concentration of particles, the higher their value. There are a number of factors, including temperature, particle size, dispersion, and stability, that influence the nanofluid's thermal conductivity [103].

4.4. Imapet of the Nanoparticles in Cavities

When it comes to solving a variety of engineering challenges, nanoparticles play an essential function in increasing heat transmission. The selection of nanoparticles to be carried by the nanofluid flow results in the highest possible rate of heat transmission. Waini and colleagues [84] investigated the effects that nanoparticles have on the flow of fluid and the transfer of heat. The authors were able to realize the flow of the Al_2O_3 -water nanofluid on a thin moving needle by using the model developed by Tiwari and Das. This model takes into account the Dufour and Soret effects. If the Schmidt number is 1, it means that the viscosity and the mass diffusion rates are both the same. The researchers in [81] discovered an increase in the rate of the heat transfer of nanofluids inside a porous parallelogram enclosure filled with a nanofluid. These findings were the subject of a numerical study using copper and alumina nanoparticles, and the researchers discovered that the presence of nanoparticles decreases the rate of heat transfer in all of the scenarios that were studied. When applied to porous media, as shown in Figure 7, the nanofluid does not give the greatest amount of heat transmission. This is demonstrated by the given fact.

The use of nanofluids is not adequate for applications involving heat transmission in porous media. It is also possible to see that the increase in heat conductivity of the porous matrix is accompanied by a decrease in the matrix's porosity. Nevertheless, the rate at which the heat transfer is reduced would increase with a reduction in both the tilt angle and the aspect ratio. On the other hand, one may also see that an increase in the thermal conductivity of the porous matrix is accompanied by a decrease in the porosity of the matrix. However, a decrease in the tilt angle and an increase in the aspect ratio would result in a faster rate of heat transfer.

Processes 2023, 11, 834 16 of 24

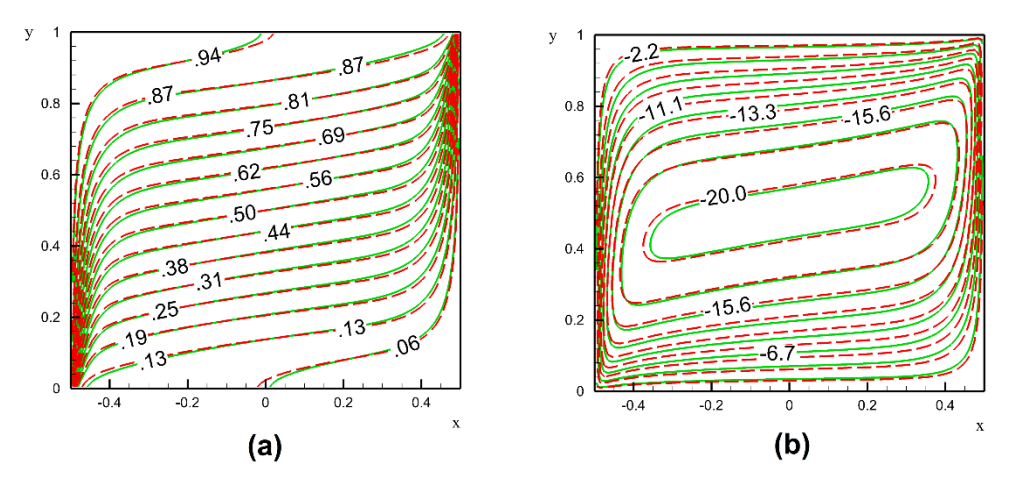


Figure 7. Effect of nanoparticles on heat transfer in porous media (a) case 1, (b) case 2 [81]. The subfigure a and b represent the behavior of nanoparticles in porous media in two different cases.

The author in [84] examines the heat transfer problem by natural convection, identifies the effects of aluminum foam, glass beads, and Cu nanoparticles, and indicates that nanoparticles in nanofluids can the improve heat transfer performance. Copper nanoparticles perform better than other nanoparticles because Cu has higher thermal conductivity than the other three nanoparticles; this enhances heat transmission in the given problem.

The authors in [89] examine the ongoing von Kármán disc problem by conducting rotary flow and heat transfer investigations of water-based magnetic nanofluids in the presence of viscous dissipation while ferrofluid is present in the space above the spinning disc. According to the findings of this study, increasing the solid volume percentage of the ferromagnetic particles leads to an increase in the rate of heat transmission through the wall. This was determined by analyzing the results of the study. In addition to this, the addition of ferromagnetic particles to water raises the convective heat transfer coefficient. The researchers in [93], investigate the free convection flow of an electrically conductive nanofluid in the vicinity of a downward-pointing spinning vertical cone when a transverse magnetic field is present. In a comparison of several nanofluids, the copper-water nanofluid was shown to have the highest skin friction coefficient and local Nusselt number. This was due to the fact that copper had the highest thermal conductivity, which is why it offers the best possible rate of heat transfer.

Finally, the nanoparticles' role in improving heat transfer is also very significant because of the way they behave thermophysically. For example, in the Tiwari and Das model for different nanofluid flow problems with different geometries, copper nanoparticles have the highest heat transfer rate compared to the other nanoparticles. Furthermore, adding a magnetic field to the nanoparticles also gives the highest rate of heat transfer improvement.

4.5. Impact of the Inclined Cavities

The use of cavities and various geometries has become increasingly crucial in nanofluids and hybrid nanofluids in recent years as the different shapes and structures of the geometry alter the flow direction and significantly affect the physical conditions of the problem, thereby assisting in achieving the desired results. The researchers used various cavities and geometries such as square, rectangular, triangular, vertical plate, channel, and trapezoidal to observe the effect of heat transfer and achieved fruitful results in controlling the temperature in buildings and in cooling technology, solar collectors, and cooling electronic equipment. The geometry of holes is crucial when it comes to increasing heat transmission in nanofluid flow. It will improve the numerical convergence of the system. This attribute pushes researchers to examine the varied cavities (geometries) for heat transfer efficiency in order to improve heat transmission efficiency. It has been demonstrated that using an inclined porous square cavity [104] in a nanofluid flow can significantly increase the amount of heat transmitted if the heater installation and inclination angle with

Processes 2023, 11, 834 17 of 24

of inclination angle in the heat transfer enhancement is described in Figure 8. State 2 State 1 State 3 0.0055 0.005 0.005 0.005 0.0045 0.004 0.004 0.004 0.0035 0.0035 0.0035 0.003 0.003 0.0025 0.0025 0.0025 0.002 0.0015 0.002 0.0015 0.002 0.0015 0.001 0.001 0.0005 0.0005 $Nu_{avg} = 20.238$ $Nu_{avg} = 20.911$ $Nu_{avg} = 20.926$ 0.006 0.0055 0.005 0.0055 0.0055 0.005 0.0045 0.004 0.005 0.0045 0.0045 0.004 0.0035 0.0035 0.0035 0.003 0.0025 0.003 0.003 0.0025 0.0025 0.0025 0.002 0.0015 0.001 0.0005 0.002 0.002 0.0015 0.001 0.002 0.0015 0.001 0.0005 0.0005 $Nu_{avg} = 21.647$ $Nu_{avg} = 19.849$ $Nu_{avg} = 21.236$ 0.0055 0.0055 0.005 0.005 0.005 0.0045 0.0045 0.0045 0.0045 0.0035 0.004 0.004 0.0035 0.003 0.0035 0.003 0.0025 0.003 0.0025 0.0025 0.002 0.0015 0.002 0.002 0.0015 0.001 0.0015 0.001 0.0005 Nu avg= 19.27 $Nu_{avg} = 15.688$ $Nu_{avg} = 20.42$ 0.006 0.0055 0.005 0.005 0.005 0.0045 0.0045 0.004 0.004 0.004 0.0035 0.0035 0.0035 0.003 0.003 0.0025 0.0025 0.002 0.002 0.002 0.0015 0.0015

regard to the nanofluid concentration and porous media are appropriately located. The use

Figure 8. Effect of inclination angle on heat transfer in the square cavity [104].

 $Nu_{avg} = 18.192$

0.001

 $Nu_{avg} = 19.488$

0.0005

According to Figure 8, the largest amount of heat transfer occurs at an angle of 0 degrees, whereas the lowest amount of heat transfer is recorded at an inclination angle of 60 degrees. However, it is feasible for an inclined cavity with side wall heating to lead to enhanced heat transfer rates when the convection effects are more prominent than the conduction effects. The angle of the cavity should be 30 degrees to 0 degrees. Another aspect of heat transmission events being investigated by researchers [86] is an inclined wavy hollow. The influence that the cavity's inclination angle has on the rate at which heat is transferred is shown in Figure 9.

0.001 0.0005

0.001

0.0005

 $Nu_{avg} = 17.074$

The angle at which the cavity is tilted is an excellent control parameter that can improve how heat is distributed. Except for the case in which the angle is 45 degrees, the average Nusselt number goes down whenever the nanoparticle volume fraction is up. The processes of heat transport have also been investigated by researchers [105] using a slanted square cavity. The impact on the circulation of heat is depicted in Figure 10.

Processes 2023, 11, 834 18 of 24

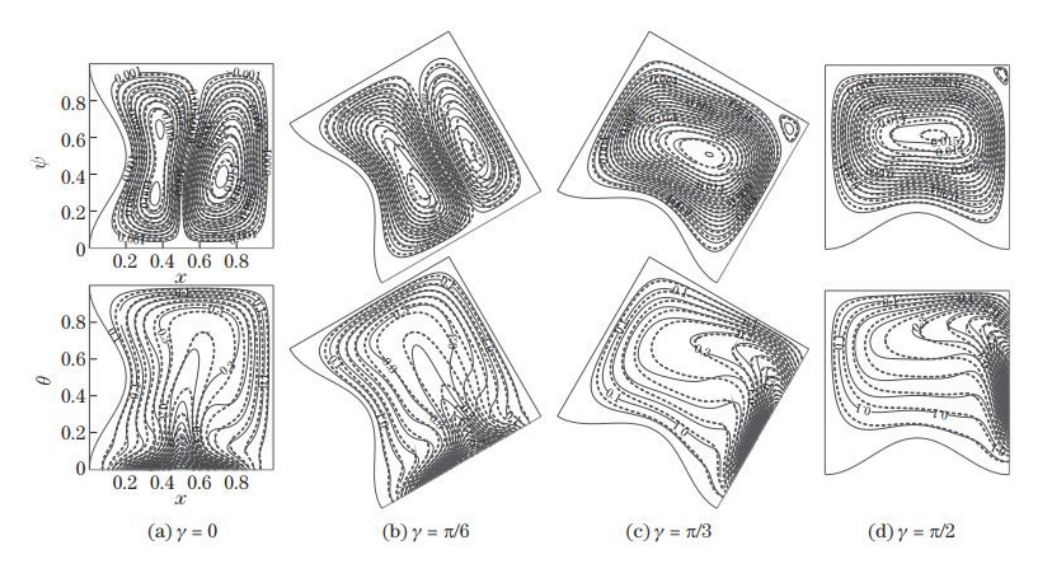


Figure 9. Effect of the inclined cavity on heat transfer [85].

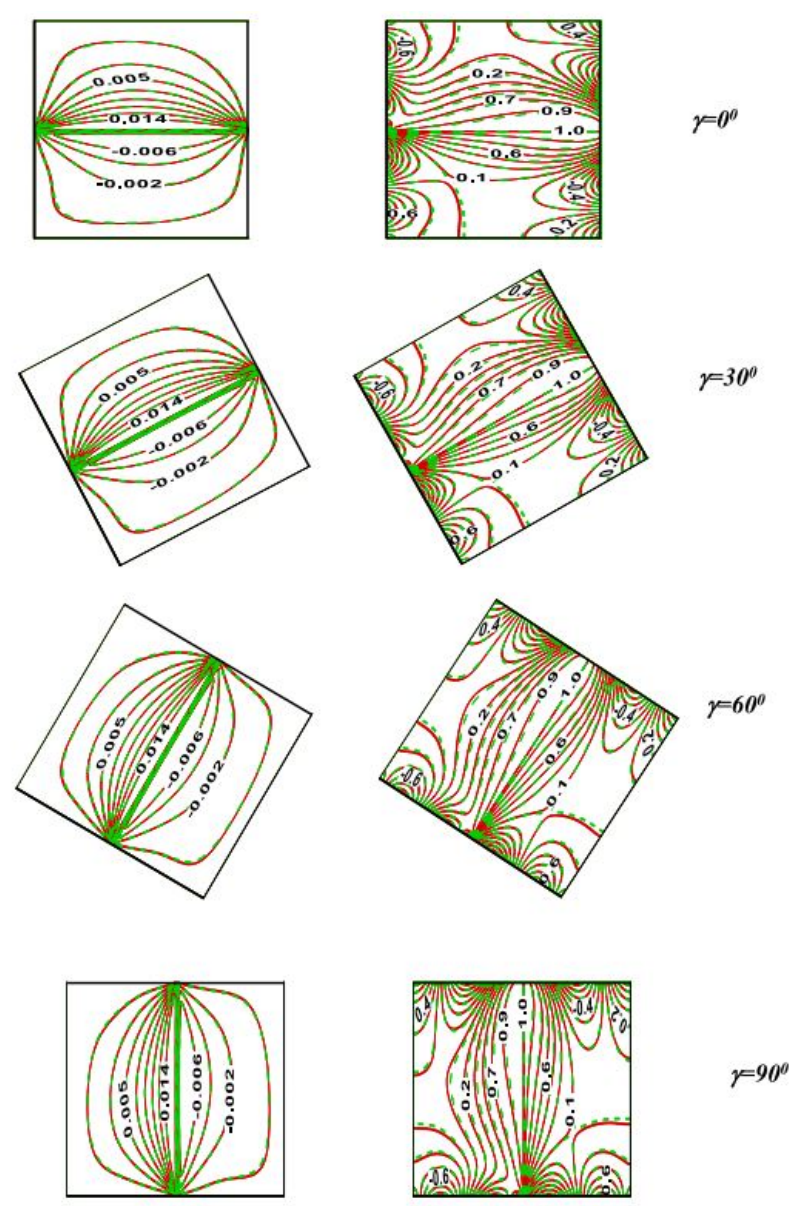


Figure 10. Effect of the inclined cavity on heat transfer [104].

Processes 2023, 11, 834 19 of 24

The inclination angle reveals a vibrant factor that significantly impacts the cavity's flow fields and temperature lines. The streamlines of the fluid inside the cavity are nearly stationary for the average angle of inclination ($0^{\circ} \le \theta \le 60^{\circ}$). At a high Ri, the impact of the inclination angle is generally observed in the temperature distribution and the fluid flow.

In conclusion, the angle of inclination of the cavity and the periodic thermal boundary conditions are both effective means of controlling the parameters that govern the movement of heat and fluid inside the cavity.

5. Future Recommendations

Several recommendations for future research efforts are made considering the literature review. According to the study, the Tiwari and Das nanofluid mathematical model and the cavities can be used to analyze heat transmission in various ways. Therefore, the following recommendations for future research are made:

- In the future, the mathematical model developed by Tiwari and Das can be extended to include thermal energy storage systems based on nanofluids.
- In the future, the Tiwari and Das single-phase model can be extended for the applications of solar collectors and the microchannel heat exchanger, along with the use of square cavities for entropy generation.
- Because the literature indicates that copper, aluminum, and titanium are the most frequently employed nanoparticles, it is proposed that additional nanoparticles be explored to achieve maximum heat transmission.
- The angle of inclination of the cavity and the periodic thermal boundary conditions can
 control the flow of heat and fluid inside the cavity; it is recommended to use inclined
 cavities in the cooling of nuclear reactors and in buildings to maintain temperature.
 Tilted cavities can also be used to control the flow of heat and fluid outside of the cavity.
- The recent years have seen more research on synthesizing and the thermophysical
 properties of hybrid nanofluids. The free convection of hybrid nanofluids in cavity
 flow has been investigated minimally. It is suggested that the Tiwari and Das model
 for free convection hybrid nanofluids be extended to include the application of solar
 collectors and drug delivery applications.

6. Conclusions

The current report provides a comprehensive overview of the research advances made in increasing convective heat transfer employing various cavities and geometries based on the Tiwari and Das nanofluid mathematical model. According to the reviewed literature, nanofluids and hybrid nanofluids offer a more significant potential for cooling, thermal storage, solar energy components, heat exchangers, and cooling-related technologies. The following closing statements are made considering the present review:

- Furthermore, it is established that copper nanoparticles provide the maximum heat transmission rate.
- The highest possible rate of heat transfer can be achieved in a variety of applications by combining hybrid nanofluids with cavities and geometries. This boosts the thermal conductivity of the nanoparticles.
- It is observed that aluminium and copper nanoparticles provide better heat transfer rates in the cavity using the Tiwari and Das nanofluid model. When compared to the base fluid, the Al₂O₃/water nanofluid's performance is improved by 6.09%.
- The inclination angle of the cavity as well as the periodic thermal boundary conditions
 can be used to effectively manage the parameters for heat and fluid flow inside
 the cavity.

Processes 2023, 11, 834 20 of 24

Author Contributions: Formal analysis, M.Z., A.H., J.A.K., M.I., Z.S., A.A.-Y. and F.A.; Writing—original draft, M.Z.; Writing—review & editing, M.Z., H.S., M.S., I.B.D., R.N., J.A.K., M.I., Z.S. and A.A.-Y.; Supervision, H.S., M.S., I.B.D. and R.N.; Methodology, A.H.; Validation, J.A.K., M.I., Z.S. and A.A.-Y.; Investigation, F.A. All authors contributed equally. All authors have read and agreed to the published version of the manuscript.

Funding: This research is funded by Yayasan Universiti Teknologi Petronas (YUTP) grant under grant cost centers [015LC0-287].

Acknowledgments: The authors thank the Department of Fundamental and Applied Science at Universiti Teknologi PETRONAS (UTP) for their assistance and support. This project was funded by grant cost center 015LC0-287 from Yayasan YUTP. Moreover, this work is also supported under the Yayasan Universiti Teknologi Petronas (YUTP) grant under grant cost centers [015LC0-272], and National Collaborative Research Fund under grant cost center [015MC0-035].

Conflicts of Interest: The authors declare no conflict of interest.

References

- 1. Wen, D.; Lin, G.; Vafaei, S.; Zhang, K. Review of nanofluids for heat transfer applications. Particuology 2009, 7, 141–150. [CrossRef]
- 2. Al-Yaari, A.; Ching, D.L.C.; Sakidin, H.; Muthuvalu, M.S.; Zafar, M.; Alyousifi, Y.; Saeed, A.A.; Haruna, A. Optimum Volume Fraction and Inlet Temperature of an Ideal Nanoparticle for Enhanced Oil Recovery by Nanofluid Flooding in a Porous Medium. *Processes* 2023, 11, 401. [CrossRef]
- 3. Hussain, A.; Muthuvalu, M.S.; Faye, I.; Ali, M.K.M.; Lebelo, R.S. Numerical Study of Glioma Growth Model with Treatment Using the Two-Stage Gauss-Seidel Method. *J. Phys. Conf. Ser.* **2018**, 1123. [CrossRef]
- 4. Hussain, A.; Muthuvalu, M.S.; Faye, I. Numerical simulation of brain tumor growth model using two-stage Gauss-Seidel method. *J. Fundam. Appl. Sci.* **2018**, *9*, 227. [CrossRef]
- Hussain, A.; Faye, I.; Muthuvalu, M.S. Performance analysis of successive over relaxation method for solving glioma growth model. AIP Conf. Proc. 2016, 1787, 020001. [CrossRef]
- 6. Hussain, A.; Faye, I.; Muthuvalu, M.S.; Boon, T.T. Least Square QR Decomposition Method for Solving the Inverse Problem in Functional Near Infra-Red Spectroscopy. In Proceedings of the 2021 IEEE 19th Student Conference on Research and Development (SCOReD), Kota Kinabalu, Malaysia, 23–25 November 2021; pp. 362–366. [CrossRef]
- 7. Abro, G.E.M.; Kakar, G.K.; Kumar, R.; Zafar, M. Maximum Power Point Tracking Using Perturb & Observe Algorithm For Hybrid Energy Generation. *J. Indep. Stud. Res. Comput.* **2021**, *18*, 1–7.
- 8. Afzal, F.; Mehmood, A.; Al Ghour, S.; Zafar, M.; Sakidin, H.; Gul, S. Characterization of Bipolar Vague Soft-Open Sets. *J. Funct. Spaces* **2022**, 2022, 5964872. [CrossRef]
- 9. Al-Yaari, A.; Ching, D.L.C.; Sakidin, H.; Muthuvalu, M.S.; Zafar, M.; Alyousifi, Y.; Saeed, A.A.H.; Bilad, M.R. Thermophysical Properties of Nanofluid in Two-Phase Fluid Flow through a Porous Rectangular Medium for Enhanced Oil Recovery. *Nanomaterials* **2022**, *12*, 1011. [CrossRef]
- 10. Al-Yaari, A.; Sakidin, H.; Zainuddin, N.; Hashim, I. Unsteady Nanofluid Flow Over Exponentially Stretching Sheet with Vertical Throughflow. In Proceedings of the 6th International Conference on Fundamental and Applied Sciences, Kuching, Malaysia, 14–16 July 2020; Springer: Berlin/Heidelberg, Germany, 2021; pp. 595–609.
- 11. Sheremet, M.A.; Grosan, T.; Pop, I. Free Convection in a Square Cavity Filled with a Porous Medium Saturated by Nanofluid Using Tiwari and Das' Nanofluid Model. *Transp. Porous Media* **2014**, *106*, 595–610. [CrossRef]
- 12. Rashad, A.M.; Gorla, R.S.R.; Mansour, M.A.; Ahmed, S.E. Magnetohydrodynamic effect on natural convection in a cavity filled with a porous medium saturated with nanofluid. *J. Porous Media* **2017**, *20*, 363–379. [CrossRef]
- 13. Sheremet, M.A.; Pop, I.; Roşca, N.C. Magnetic field effect on the unsteady natural convection in a wavy-walled cavity filled with a nanofluid: Buongiorno's mathematical model. *J. Taiwan Inst. Chem. Eng.* **2016**, *61*, 211–222. [CrossRef]
- 14. Kefayati, G. Heat transfer and entropy generation of natural convection on non-Newtonian nanofluids in a porous cavity. *Powder Technol.* **2016**, 299, 127–149. [CrossRef]
- 15. Sheremet, M.A.; Pop, I. Free convection in a triangular cavity filled with a porous medium saturated by a nanofluid: Buongiorno's mathematical model. *Int. J. Num. Methods Heat Fluid Flow* **2015**, 25, 1138–1161. [CrossRef]
- 16. Astanina, M.S.; Sheremet, M.A.; Oztop, H.F.; Abu-Hamdeh, N. MHD natural convection and entropy generation of ferrofluid in an open trapezoidal cavity partially filled with a porous medium. *Int. J. Mech. Sci.* **2018**, *136*, 493–502. [CrossRef]
- 17. Selimefendigil, F.; Öztop, H.F.; Chamkha, A.J. MHD mixed convection and entropy generation of nanofluid filled lid driven cavity under the influence of inclined magnetic fields imposed to its upper and lower diagonal triangular domains. *J. Magn. Magn. Mater.* **2016**, 406, 266–281. [CrossRef]
- 18. Sheremet, M.; Oztop, H.; Pop, I. MHD natural convection in an inclined wavy cavity with corner heater filled with a nanofluid. *J. Magn. Magn. Mater.* **2016**, 416, 37–47. [CrossRef]
- 19. Hoghoughi, G.; Izadi, M.; Oztop, H.F.; Abu-Hamdeh, N. Effect of geometrical parameters on natural convection in a porous undulant-wall enclosure saturated by a nanofluid using Buongiorno's model. *J. Mol. Liq.* **2018**, 255, 148–159. [CrossRef]

Processes 2023, 11, 834 21 of 24

20. Sheikholeslami, M. Influence of magnetic field on nanofluid free convection in an open porous cavity by means of Lattice Boltzmann method. *J. Mol. Liq.* **2017**, 234, 364–374. [CrossRef]

- 21. Rashad, A.; Rashidi, M.; Lorenzini, G.; Ahmed, S.E.; Aly, A.M. Magnetic field and internal heat generation effects on the free convection in a rectangular cavity filled with a porous medium saturated with Cu–water nanofluid. *Int. J. Heat Mass Transf.* **2017**, 104, 878–889. [CrossRef]
- Ghasemi, K.; Siavashi, M. Lattice Boltzmann numerical simulation and entropy generation analysis of natural convection of nanofluid in a porous cavity with different linear temperature distributions on side walls. *J. Mol. Liq.* 2017, 233, 415–430.
 [CrossRef]
- 23. Sheikholeslami, M. Magnetohydrodynamic nanofluid forced convection in a porous lid driven cubic cavity using Lattice Boltzmann method. *J. Mol. Liq.* **2017**, 231, 555–565. [CrossRef]
- 24. Sheikholeslami, M. Influence of magnetic field on Al2O3-H2O nanofluid forced convection heat transfer in a porous lid driven cavity with hot sphere obstacle by means of LBM. *J. Mol. Liq.* **2018**, *263*, *472*–488. [CrossRef]
- 25. Sheikholeslami, M. Magnetic field influence on CuO–H₂O nanofluid convective flow in a permeable cavity considering various shapes for nanoparticles. *Int. J. Hydrogen Energy* **2017**, 42, 19611–19621. [CrossRef]
- 26. Haq, R.U.; Soomro, F.A.; Mekkaoui, T.; Al-Mdallal, Q.M. MHD natural convection flow enclosure in a corrugated cavity filled with a porous medium. *Int. J. Heat Mass Transf.* **2018**, *121*, 1168–1178. [CrossRef]
- Mehryan, S.; Izadi, M.; Sheremet, M.A. Analysis of conjugate natural convection within a porous square enclosure occupied with micropolar nanofluid using local thermal non-equilibrium model. J. Mol. Liq. 2018, 250, 353–368. [CrossRef]
- 28. Basak, T.; Chamkha, A.J. Heatline analysis on natural convection for nanofluids confined within square cavities with various thermal boundary conditions. *Int. J. Heat Mass Transf.* **2012**, *55*, 5526–5543. [CrossRef]
- 29. Zhou, Y.; Rajapakse, R.; Graham, J. Coupled consolidation of a porous medium with a cylindrical or a spherical cavity. *Int. J. Numer. Anal. Methods Géoméch.* **1998**, 22, 449–475. [CrossRef]
- 30. Toosi, M.H.; Siavashi, M. Two-phase mixture numerical simulation of natural convection of nanofluid flow in a cavity partially filled with porous media to enhance heat transfer. *J. Mol. Liq.* **2017**, 238, 553–569. [CrossRef]
- 31. Kefayati, G. Simulation of natural convection and entropy generation of non-Newtonian nanofluid in a porous cavity using Buongiorno's mathematical model. *Int. J. Heat Mass Transf.* **2017**, *112*, 709–744. [CrossRef]
- 32. Javed, T.; Mehmood, Z.; Abbas, Z. Natural convection in square cavity filled with ferrofluid saturated porous medium in the presence of uniform magnetic field. *Phys. B Condens. Matter* **2017**, *506*, 122–132. [CrossRef]
- 33. Kefayati, G. Natural convection of ferrofluid in a linearly heated cavity utilizing LBM. J. Mol. Liq. 2014, 191, 1–9. [CrossRef]
- 34. Basak, T.; Roy, S.; Takhar, H.S. Effects of Nonuniformly Heated Wall(S) on a Natural-Convection Flow in a Square Cavity Filled with a Porous Medium. *Numer. Heat Transf. Part A Appl.* **2007**, *51*, 959–978. [CrossRef]
- 35. Baytaş, A. Entropy generation for natural convection in an inclined porous cavity. *Int. J. Heat Mass Transf.* **2000**, *43*, 2089–2099. [CrossRef]
- 36. Kefayati, G.R. Lattice Boltzmann simulation of MHD natural convection in a nanofluid-filled cavity with sinusoidal temperature distribution. *Powder Technol.* **2013**, 243, 171–183. [CrossRef]
- 37. Sheremet, M.; Pop, I.; Bachok, N. Effect of thermal dispersion on transient natural convection in a wavy-walled porous cavity filled with a nanofluid: Tiwari and Das' nanofluid model. *Int. J. Heat Mass Transf.* **2016**, 92, 1053–1060. [CrossRef]
- 38. Astanina, M.S.; Sheremet, M.A.; Umavathi, J.C. Unsteady Natural Convection with Temperature-Dependent Viscosity in a Square Cavity Filled with a Porous Medium. *Transp. Porous Media* **2015**, *110*, 113–126. [CrossRef]
- 39. Sheremet, M.A.; Pop, I. Natural Convection in a Square Porous Cavity with Sinusoidal Temperature Distributions on Both Side Walls Filled with a Nanofluid: Buongiorno's Mathematical Model. *Transp. Porous Media* **2014**, *105*, 411–429. [CrossRef]
- 40. Sivasankaran, S.; Mansour, M.A.; Rashad, A.M.; Bhuvaneswari, M. MHD mixed convection of Cu–water nanofluid in a two-sided lid-driven porous cavity with a partial slip. *Numer. Heat Transf. Part A Appl.* **2016**, *70*, 1356–1370. [CrossRef]
- 41. Ghalambaz, M.; Sabour, M.; Pop, I. Free convection in a square cavity filled by a porous medium saturated by a nanofluid: Viscous dissipation and radiation effects. *Eng. Sci. Technol. Int. J.* **2016**, *19*, 1244–1253. [CrossRef]
- 42. Maghsoudi, P.; Siavashi, M. Application of nanofluid and optimization of pore size arrangement of heterogeneous porous media to enhance mixed convection inside a two-sided lid-driven cavity. *J. Therm. Anal. Calorim.* **2019**, *135*, 947–961. [CrossRef]
- 43. Tahmasebi, A.; Mahdavi, M.; Ghalambaz, M. Local thermal nonequilibrium conjugate natural convection heat transfer of nanofluids in a cavity partially filled with porous media using Buongiorno's model. *Numer. Heat Transf. Part A Appl.* **2018**, 73, 254–276. [CrossRef]
- 44. Mehmood, K.; Hussain, S.; Sagheer, M. Numerical simulation of MHD mixed convection in alumina–water nanofluid filled square porous cavity using KKL model: Effects of non-linear thermal radiation and inclined magnetic field. *J. Mol. Liq.* **2017**, 238, 485–498. [CrossRef]
- 45. Ullah, N.; Nadeem, S.; Khan, A.U. Finite element simulations for natural convective flow of nanofluid in a rectangular cavity having corrugated heated rods. *J. Therm. Anal. Calorim.* **2021**, *143*, 4169–4181. [CrossRef]
- 46. Ahmed, S.E.; Aly, A.M. Mixed convection in a nanofluid-filled sloshing porous cavity including inner heated rose. *J. Therm. Anal. Calorim.* **2021**, 143, 275–291. [CrossRef]
- 47. Jing, D.; Hu, S.; Hatami, M.; Xiao, Y.; Jia, J. Thermal analysis on a nanofluid-filled rectangular cavity with heated fins of different geometries under magnetic field effects. *J. Therm. Anal. Calorim.* **2020**, *139*, 3577–3588. [CrossRef]

Processes 2023, 11, 834 22 of 24

48. Molana, M.; Dogonchi, A.; Armaghani, T.; Chamkha, A.J.; Ganji, D.; Tlili, I. Investigation of Hydrothermal Behavior of Fe₃O₄-H₂O Nanofluid Natural Convection in a Novel Shape of Porous Cavity Subjected to Magnetic Field Dependent (MFD) Viscosity. *J. Energy Storage* **2020**, *30*, 101395. [CrossRef]

- 49. Zafar, M.; Sakidin, H.; Dzulkarnain, I.; Afzal, F. Numerical Investigations of Nano-fluid Flow in Square Porous Cavity: Buongiorno's Mathematical Model. In Proceedings of the 6th International Conference on Fundamental and Applied Sciences, Kuching, Malaysia, 14–16 July 2020; Springer: Berlin/Heidelberg, Germany, 2021; pp. 739–748. [CrossRef]
- 50. Javadzadegan, A.; Joshaghani, M.; Moshfegh, A.; Akbari, O.A.; Afrouzi, H.H.; Toghraie, D. Accurate meso-scale simulation of mixed convective heat transfer in a porous media for a vented square with hot elliptic obstacle: An LBM approach. *Phys. A Stat. Mech. Appl.* **2020**, 537, 122439. [CrossRef]
- 51. Ram, D.; Bhandari, D.S.; Tripathi, D.; Sharma, K. Propagation of H1N1 virus through saliva movement in oesophagus: A mathematical model. *Eur. Phys. J. Plus* **2022**, *137*, 1–11. [CrossRef]
- 52. Vijay, N.; Sharma, K. Heat and mass transfer study of ferrofluid flow between co-rotating stretchable disks with geothermal viscosity: HAM analysis. *Chin. J. Phys.* **2022**, *78*, 83–95. [CrossRef]
- 53. Kumar, S.; Sharma, K. Impacts of Stefan Blowing on Reiner–Rivlin Fluid Flow Over Moving Rotating Disk with Chemical Reaction. *Arab. J. Sci. Eng.* **2022**, 1–10. [CrossRef]
- 54. Kefayati, G. Mixed convection of non-Newtonian nanofluid in an enclosure using Buongiorno's mathematical model. *Int. J. Heat Mass Transf.* **2017**, *108*, 1481–1500. [CrossRef]
- 55. Ahmed, S.E.; Oztop, H.F.; Al-Salem, K. Natural convection coupled with radiation heat transfer in an inclined porous cavity with corner heater. *Comput. Fluids* **2014**, *102*, 74–84. [CrossRef]
- 56. Oztop, H.F.; Al-Salem, K.; Pop, I. MHD mixed convection in a lid-driven cavity with corner heater. *Int. J. Heat Mass Transf.* **2011**, 54, 3494–3504. [CrossRef]
- 57. Sreedevi, P.; Reddy, P.S. Effect of magnetic field and thermal radiation on natural convection in a square cavity filled with TiO₂ nanoparticles using Tiwari-Das nanofluid model. *Alex. Eng. J.* **2022**, *61*, 1529–1541. [CrossRef]
- 58. Bondareva, N.S.; Sheremet, M.A.; Oztop, H.F.; Abu-Hamdeh, N. Entropy generation due to natural convection of a nanofluid in a partially open triangular cavity. *Adv. Powder Technol.* **2017**, *28*, 244–255. [CrossRef]
- 59. Oliveski, R.D.C.; Macagnan, M.H.; Copetti, J.B. Entropy generation and natural convection in rectangular cavities. *Appl. Therm. Eng.* **2009**, 29, 1417–1425. [CrossRef]
- 60. Marzougui, S.; Mebarek-Oudina, F.; Assia, A.; Magherbi, M.; Shah, Z.; Ramesh, K. Entropy generation on magneto-convective flow of copper–water nanofluid in a cavity with chamfers. *J. Therm. Anal. Calorim.* **2020**, *143*, 2203–2214. [CrossRef]
- 61. Bejan, A. Second law analysis in heat transfer. Energy 1980, 5, 720–732. [CrossRef]
- 62. Oztop, H.F.; Al-Salem, K. A review on entropy generation in natural and mixed convection heat transfer for energy systems. *Renew. Sustain. Energy Rev.* **2012**, *16*, 911–920. [CrossRef]
- 63. Awais, M.; Ullah, N.; Ahmad, J.; Sikandar, F.; Ehsan, M.M.; Salehin, S.; Bhuiyan, A.A. Heat transfer and pressure drop performance of Nanofluid: A state-of- the-art review. *Int. J. Thermofluids* **2021**, *9*, 100065. [CrossRef]
- 64. Bakthavatchalam, B.; Habib, K.; Saidur, R.; Saha, B.B.; Irshad, K. Comprehensive study on nanofluid and ionanofluid for heat transfer enhancement: A review on current and future perspective. *J. Mol. Liq.* **2020**, *305*, 112787. [CrossRef]
- 65. Liang, G.; Mudawar, I. Review of single-phase and two-phase nanofluid heat transfer in macro-channels and micro-channels. *Int. J. Heat Mass Transf.* **2019**, 136, 324–354. [CrossRef]
- 66. Sheikholeslami, M.; Rokni, H.B. Simulation of nanofluid heat transfer in presence of magnetic field: A review. *Int. J. Heat Mass Transf.* **2017**, *115*, 1203–1233. [CrossRef]
- 67. Okonkwo, E.C.; Wole-Osho, I.; Almanassra, I.W.; Abdullatif, Y.M.; Al-Ansari, T. An updated review of nanofluids in various heat transfer devices. *J. Therm. Anal. Calorim.* **2021**, *145*, 2817–2872. [CrossRef]
- 68. Khan, U.; Zaib, A.; Pop, I.; Waini, I.; Ishak, A. MHD flow of a nanofluid due to a nonlinear stretching/shrinking sheet with a convective boundary condition: Tiwari–Das nanofluid model. *Int. J. Numer. Methods Heat Fluid Flow* **2022**, 32, 3233–3258. [CrossRef]
- 69. Jamshed, W.; Kumar, V.; Kumar, V. Computational examination of Casson nanofluid due to a non-linear stretching sheet subjected to particle shape factor: Tiwari and Das model. *Numer. Methods Partial. Differ. Equ.* **2022**, *38*, 848–875. [CrossRef]
- 70. Buongiorno, J. Convective Transport in Nanofluids. J. Heat Transfer. 2006, 128, 240–250. [CrossRef]
- 71. Vafai, K. Handbook of Porous Media; CRC Press: Boca Raton, FL, USA, 2015.
- 72. Tiwari, R.K.; Das, M.K. Heat transfer augmentation in a two-sided lid-driven differentially heated square cavity utilizing nanofluids. *Int. J. Heat Mass Transf.* **2007**, *50*, 2002–2018. [CrossRef]
- 73. Rashad, A.M.; Mansour, M.A.; Armaghani, T.; Chamkha, A.J. MHD mixed convection and entropy generation of nanofluid in a lid-driven U-shaped cavity with internal heat and partial slip. *Phys. Fluids* **2019**, *31*, 042006. [CrossRef]
- 74. Nayak, R.; Bhattacharyya, S.; Pop, I. Numerical study on mixed convection and entropy generation of Cu–water nanofluid in a differentially heated skewed enclosure. *Int. J. Heat Mass Transf.* **2015**, *85*, 620–634. [CrossRef]
- 75. Nayak, R.K.; Bhattacharyya, S.; Pop, I. Numerical Study on Mixed Convection and Entropy Generation of a Nanofluid in a Lid-Driven Square Enclosure. *J. Heat Transf.* **2015**, *138*, 012503. [CrossRef]
- 76. Ting, K.; Mozumder, A.K.; Das, P.K. Effect of surface roughness on heat transfer and entropy generation of mixed convection in nanofluid. *Phys. Fluids* **2019**, *31*, 093602. [CrossRef]

Processes 2023, 11, 834 23 of 24

77. Sheremet, M.; Pop, I.; Öztop, H.F.; Abu-Hamdeh, N. Natural convection of nanofluid inside a wavy cavity with a non-uniform heating. *Int. J. Numer. Methods Heat Fluid Flow* **2017**, 27, 958–980. [CrossRef]

- 78. Rohde, L.E.; Clausell, N.; Ribeiro, J.P.; Goldraich, L.; Netto, R.; Dec, G.W.; DiSalvo, T.G.; Polanczyk, C.A. Health outcomes in decompensated congestive heart failure: A comparison of tertiary hospitals in Brazil and United States. *Int. J. Cardiol.* **2005**, 102, 71–77. [CrossRef]
- 79. Sreedevi, P.; Reddy, P.S.; Rao, K.V.S. Effect of magnetic field and radiation on heat transfer analysis of nanofluid inside a square cavity filled with silver nanoparticles: Tiwari–Das model. *Waves Random Complex Media* **2021**, 1–19. [CrossRef]
- 80. Sheremet, M.A.; Grosan, T.; Pop, I. Thermal convection in a chamber filled with a nanosuspension driven by a chemical reaction using Tiwari and Das' model. *Int. J. Numer. Methods Heat Fluid Flow* **2020**, *31*, 452–470. [CrossRef]
- 81. Ghalambaz, M.; Sheremet, M.A.; Pop, I. Free Convection in a Parallelogrammic Porous Cavity Filled with a Nanofluid Using Tiwari and Das' Nanofluid Model. *PLoS ONE* **2015**, *10*, e0126486. [CrossRef]
- 82. Wang, X.; Wang, J. Numerical Simulation of Natural Convection in a Triangle Cavity Filled with Nanofluids Using Tiwari and Das' Model: Effects of Heat Flux. *Heat Trans. Asian Res.* **2017**, *46*, 761–777. [CrossRef]
- 83. Sheremet, M.A.; Dinarvand, S.; Pop, I. Effect of thermal stratification on free convection in a square porous cavity filled with a nanofluid using Tiwari and Das' nanofluid model. *Phys. E Low-Dimens. Syst. Nanostruct.* **2015**, *69*, 332–341. [CrossRef]
- 84. Waini, I.; Ishak, A.; Pop, I. Dufour and Soret effects on Al₂O₃-water nanofluid flow over a moving thin needle: Tiwari and Das model. *Int. J. Numer. Methods Heat Fluid Flow* **2020**, *31*, 766–782. [CrossRef]
- 85. Selimefendigil, F.; Chamkha, A.J. Magnetohydrodynamics mixed convection in a power law nanofluid-filled triangular cavity with an opening using Tiwari and Das' nanofluid model. *J. Therm. Anal. Calorim.* **2018**, *135*, 419–436. [CrossRef]
- 86. Sheremet, M.A.; Trîmbiţaş, R.; Groşan, T.; Pop, I. Natural convection of an alumina-water nanofluid inside an inclined wavy-walled cavity with a non-uniform heating using Tiwari and Das' nanofluid model. *Appl. Math. Mech.* **2018**, *39*, 1425–1436. [CrossRef]
- 87. Yashkun, U.; Zaimi, K.; Abu Bakar, N.A.; Ferdows, M. Nanofluid Stagnation-Point Flow Using Tiwari and Das Model Over a Stretching/Shrinking Sheet with Suction and Slip Effects. *J. Adv. Res. Fluid Mech. Therm. Sci.* **2021**, *70*, 62–76. Available online: https://www.akademiabaru.com/submit/index.php/arfmts/article/view/2936 (accessed on 15 March 2022). [CrossRef]
- 88. Roşca, N.C.; Pop, I. Axisymmetric rotational stagnation point flow impinging radially a permeable stretching/shrinking surface in a nanofluid using Tiwari and Das model. Sci. Rep. 2017, 7, 40299. [CrossRef]
- 89. Mustafa, M.; Khan, J.A.; Hayat, T.; Alsaedi, A. Numerical Solutions for Radiative Heat Transfer in Ferrofluid Flow due to a Rotating Disk: Tiwari and Das Model. *Int. J. Nonlinear Sci. Numer. Simul.* **2018**, *19*, 1–10. [CrossRef]
- 90. Dinarvand, S.; Rostami, M.N. Mixed Convection of A Cu-Ag/Water Hybrid Nanofluid Along A Vertical Porous Cylinder Via Modified Tiwari–Das Model. *J. Theor. Appl. Mech.* **2019**, *49*, 149–169. [CrossRef]
- 91. Mabood, F.; Ibrahim, S.; Kumar, P.; Khan, W. Viscous dissipation effects on unsteady mixed convective stagnation point flow using Tiwari-Das nanofluid model. *Results Phys.* **2017**, *7*, 280–287. [CrossRef]
- 92. Ramreddy, C.; Muralikrishna, P. Effects of First and Second Order Velocity Slips on Melting Stretching Surface in a Thermally Stratified Nanofluid: Tiwari and Das' Model. *J. Nanofluids* **2017**, *6*, 155–163. [CrossRef]
- 93. Aghamajidi, M.; Yazdi, M.; Dinarvand, S.; Pop, I. Tiwari-Das nanofluid model for magnetohydrodynamics (MHD) natural-convective flow of a nanofluid adjacent to a spinning down-pointing vertical cone. *Propuls. Power Res.* **2018**, *7*, 78–90. [CrossRef]
- 94. Dinarvand, S.; Pop, I. Free-convective flow of copper/water nanofluid about a rotating down-pointing cone using Tiwari-Das nanofluid scheme. *Adv. Powder Technol.* **2017**, *28*, 900–909. [CrossRef]
- 95. Dinarvand, S.; Hosseini, R.; Pop, I. Axisymmetric mixed convective stagnation-point flow of a nanofluid over a vertical permeable cylinder by Tiwari-Das nanofluid model. *Powder Technol.* **2017**, *311*, 147–156. [CrossRef]
- 96. Dinarvand, S.; Hosseini, R.; Pop, I. Homotopy analysis method for unsteady mixed convective stagnation-point flow of a nanofluid using Tiwari-Das nanofluid model. *Int. J. Numer. Methods Heat Fluid Flow* **2016**, *26*, 40–62. [CrossRef]
- 97. Chen, H.; Xiao, T.; Shen, M. Nanofluid Flow in a Porous Channel with Suction and Chemical Reaction using Tiwari and Das's Nanofluid Model. *Heat Trans. Asian Res.* **2017**, *46*, 1041–1052. [CrossRef]
- 98. Das, S.K.; Putra, N.; Thiesen, P.H.; Roetzel, W. Temperature Dependence of Thermal Conductivity Enhancement for Nanofluids. *J. Heat Transf.* **2003**, 125, 567–574. [CrossRef]
- 99. Webb, R.L.; Kim, N. Enhanced Heat Transfer; Taylor and Francis: Abingdon, UK, 2005.
- 100. Xuan, Y.; Li, Q. Heat transfer enhancement of nanofluids. Int. J. Heat Fluid Flow 2000, 21, 58-64. [CrossRef]
- 101. Choi, S.U.; Eastman, J.A. Enhancing Thermal Conductivity of Fluids with Nanoparticles; Argonne National Lab.: Argonne, IL, USA, 1995.
- 102. Kristiawan, B.; Rifa'I, A.I.; Enoki, K.; Wijayanta, A.T.; Miyazaki, T. Enhancing the thermal performance of TiO₂/water nanofluids flowing in a helical microfin tube. *Powder Technol.* **2020**, *376*, 254–262. [CrossRef]
- 103. Murshed, S.; Leong, K.; Yang, C. A combined model for the effective thermal conductivity of nanofluids. *Appl. Therm. Eng.* **2009**, 29, 2477–2483. [CrossRef]

Processes 2023, 11, 834 24 of 24

104. Emami, R.Y.; Siavashi, M.; Moghaddam, G.S. The effect of inclination angle and hot wall configuration on Cu-water nanofluid natural convection inside a porous square cavity. *Adv. Powder Technol.* **2018**, *29*, 519–536. [CrossRef]

105. Begum, A.S.; Chamkha, A.J. Analysis of mixed convection in an inclined square cavity using nanofluids with Vajjha and Das' nanofluid model. *Heat Transf.* **2021**, *50*, 4744–4756. [CrossRef]

Disclaimer/Publisher's Note: The statements, opinions and data contained in all publications are solely those of the individual author(s) and contributor(s) and not of MDPI and/or the editor(s). MDPI and/or the editor(s) disclaim responsibility for any injury to people or property resulting from any ideas, methods, instructions or products referred to in the content.